



Cite this: *J. Mater. Chem. B*, 2025, **13**, 4739

## Nanostructured conductive polymers: synthesis and application in biomedicine

Tingting Cheng,<sup>ab</sup> Ying Xiang,<sup>b</sup> Xuan He,<sup>b</sup> Ji Pang,<sup>b</sup> Weihao Zhu,<sup>b</sup> Liqiang Luo,<sup>id a</sup> Yi Cao<sup>id \*b</sup> and Renjun Pei<sup>\*bc</sup>

Conductive polymers (CPs), distinguished by their  $sp^2$ -hybridized carbon backbone, offer remarkable electrical conductivity while maintaining the advantageous mechanical flexibility and processing characteristics typical of organic polymers. Compared to their bulk counterparts, nanostructured CPs exhibit unique physicochemical properties, such as large surface areas and shortened charge/mass transport pathways, making them promising candidates for various applications. This mini review explores various synthesis methodologies for nanostructured CPs, including electrospinning, hard templating, and soft templating techniques, while elucidating their advantages and disadvantages. Additionally, the burgeoning biomedical applications of nanostructured CPs are highlighted, including drug delivery, neural electrodes and interfaces, nerve regeneration, and biosensing, demonstrating their potential to significantly advance contemporary biomedical science.

Received 9th November 2024,  
Accepted 19th March 2025

DOI: 10.1039/d4tb02513j

[rsc.li/materials-b](https://rsc.li/materials-b)

### 1. Introduction

Conductive polymers (CPs) were first introduced as “synthetic metals” in the mid-1970s. These polymeric materials have conjugated bonds that can be chemically or electrochemically doped, transforming them from insulators to conductors.<sup>1–7</sup> Typical CPs mainly include polyacetylene (PA), polyaniline (PANI), polypyrrole (PPY), polythiophene (PT), and their derivatives, such as poly(3,4-ethylenedioxythiophene) (PEDOT) and poly(3-hexylthiophene) (P3HT).<sup>1,4,8,9</sup> Compared to conventional non-conductive polymers, intrinsically conductive CPs have good conductivity due to the  $sp^2$  hybridization in the main chains, which facilitates the transport charge carriers.<sup>10</sup>

In comparison with conventional bulk CPs, nanostructured CPs offer several advantages, including better homogeneity, larger specific surface area, higher porosity, enhanced mechanical properties, and greater flexibility, further extending their benefits in the fields of sensors, energy, and electronic devices. Additionally, incorporating additives during preparation is a common method for improving operability or properties of CPs. For example, blending CPs with polyethylene oxide (PEO) improves their solubility, enabling successful electrospinning

into filaments.<sup>11,12</sup> Moreover, PPY nanofibers blended with silk fibroin (SF) have shown enhanced mechanical properties and biocompatibility, making them suitable for applications in myocardial tissues.<sup>13</sup> This suggests that nanostructured CP composites not only retain their conductive properties but also offer additional advantages, expanding the potential of CPs in biomedical applications.

Several excellent books and reviews have thoroughly detailed the preparative aspects of CPs and their nanostructures,<sup>4,5,10,14</sup> as well as provided insightful discussions on the applications of CPs and their composites in energy, sensors, electronic devices, neural electrodes, and more.<sup>2,8,11–15</sup> This mini review aims to highlight the various preparation methods for nanostructured CPs, examining their advantages and disadvantages, and will focus on their latest applications in the field of biomedicine (Fig. 1).

### 2. Preparation of nanostructured CPs

CPs are widely used in many fields due to their excellent properties, and their preparation techniques have also evolved significantly. Various methods have been developed to prepare CPs with diverse structures, including nanofibers, nanotubes, nanoneedles, nanowires, and nanotunnels. In this section, we will summarize the strategies for obtaining CPs with these nanostructures, such as electrostatic spinning, hard and soft template methods, solution self-assembly, directed electrochemical nanowire assembly, and dielectric electrophoretic synthesis. A comparison of the advantages and disadvantages of these

<sup>a</sup> Department of Chemistry, College of Sciences, Shanghai University, Shanghai 200444, China

<sup>b</sup> CAS Key Laboratory of Nano-Bio Interface, Division of Nanobiomedicine, Suzhou Institute of Nano-Tech and Nano-Bionics, Chinese Academy of Sciences, Suzhou 215123, China. E-mail: ycao2014@sinano.ac.cn, rjpei2011@sinano.ac.cn; Tel: +86 0512 62872587, +86 0512 62872776

<sup>c</sup> School of Nano-Tech and Nano-Bionics, University of Science and Technology of China, Hefei 230026, China



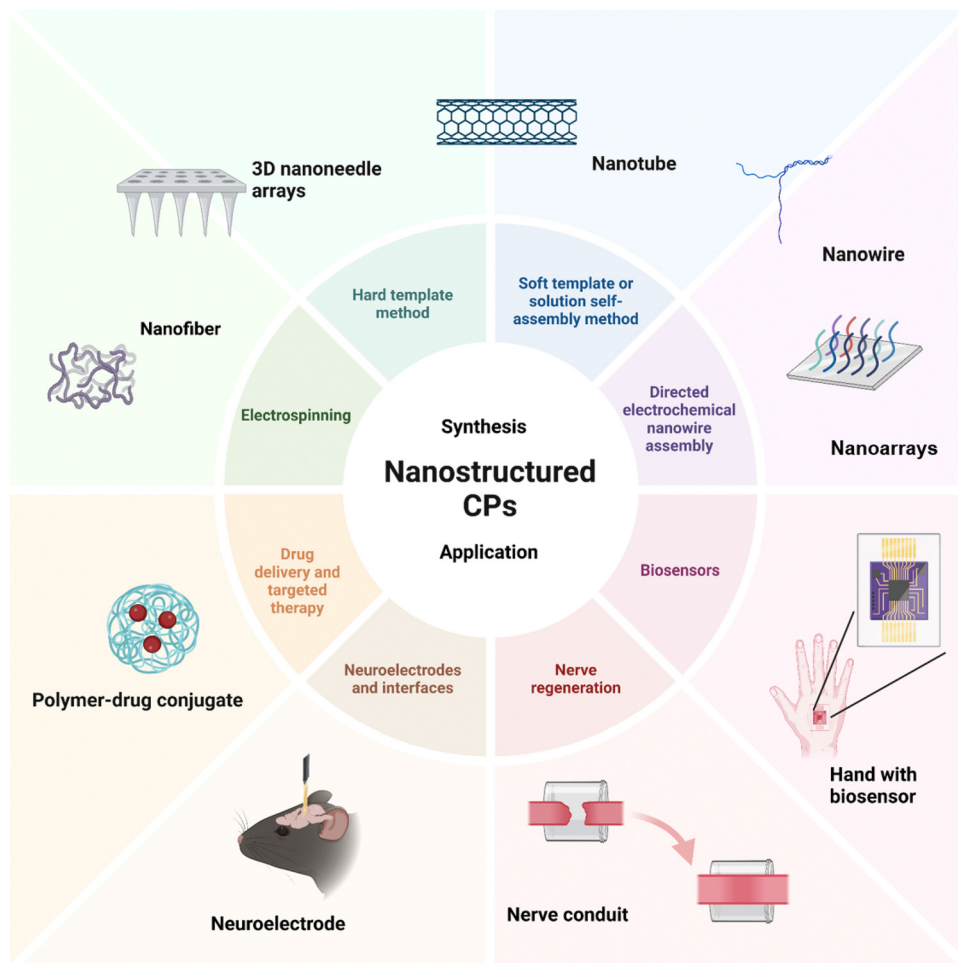


Fig. 1 Schematic illustrating the preparation of nanostructured CPs and their applications in biomedicine.

approaches for preparing nanostructured CPs can be found in Table 1.

## 2.1 Electrospinning

Electrospinning utilizes a high-voltage electrostatic field to draw nanofibers from a liquid polymer solution or melt. The liquid jet rapidly solidifies in air, forming continuous fibers. These nanofibers, possessing excellent properties, are used in textiles, filtration, insulation, and other applications.<sup>14</sup> The simplicity, efficiency, and low cost of electrospinning have led to its widespread use in textiles, medicine, and environmental protection.

Although electrospinning is regarded as a simple, versatile and cost-effective technique for producing continuous ultrafine polymer fibers, the direct electrospinning of CP fibers still faces challenges, primarily including the low solubility and intrinsic brittleness of CPs. To overcome these limitations and enhance the charge carrier mobility in electrospun CPs fibers, several strategies have been developed. In this section, we will summarize the strategies for the synthesis of nanostructured conducting compounds from four aspects: direct electrospinning of CPs into fibers, coaxial electrospinning of CPs,

co-electrospinning of CPs with other polymers, and template-assisted synthesis using electrospun fibers as templates.

**2.1.1 Direct electrospinning of CPs.** Direct electrospinning of CPs has been rarely reported, likely due to their rigid backbones, low molecular weights, and lack of suitable organic solvents for electrospinning.<sup>14</sup> High CP concentrations often result in precipitation, while low concentrations form bead-like structures rather than uniform nanofibers. Only a few soluble CPs, such as PPY,<sup>120</sup> P3HT,<sup>6,16</sup> and PANI,<sup>18,30,121</sup> have been directly electrospun. Fig. 2(A) illustrates a schematic diagram of the apparatus utilized for direct electrospinning. For instance, González *et al.*<sup>15</sup> dissolved cubic regularity P3HT in chloroform with an appropriate concentration but obtained fibers that were present with large beads after electrospinning. It should be noted that direct electrospinning of CPs allows for the addition of dopants to improve CP solubility. Yu *et al.*<sup>17</sup> successfully prepared PANI submicron fibers (Fig. 2(B) and (C)) by dissolving PANI with an appropriate molecular weight in hot sulfuric acid, though they encountered challenges with molecular weight and fiber size limitations. To address these challenges, Spiers *et al.*<sup>29</sup> used (+)-camphor-10-sulfonic acid (HCSA) doping to process high-concentration, high-molecular-weight PANI



Table 1 Advantages and disadvantages of approaches for preparing nanostructured CPs

Approach	Advantages	Disadvantages	Structure of CPs	Ref.
Electrospinning	<ul style="list-style-type: none"> <li>Simple device</li> <li>Possibility of higher electrical conductivity with pure CPs</li> <li>Scalable</li> </ul>	<ul style="list-style-type: none"> <li>Limited applicable CPs due to their typically rigid backbones, low molecular weight, and low degree of chain entanglement, making them difficult to dissolve</li> <li>May exhibit poor mechanical properties</li> <li>Poor nanofiber morphology (droplet-like or bead-like) and larger diameter</li> <li>Use of poisonous reagents</li> <li>Requirement of special device (coaxial needle)</li> <li>Modifying some additional parameters compared to normal electrospinning</li> <li>Use of poisonous reagents</li> <li>Introduction of insulating blends polymers reducing the overall conductivity of CPs</li> </ul>	P3HT, PANI, and PPY nanofiber	6, 15–18
	<ul style="list-style-type: none"> <li>Possibility of removing non-conductive parts after electrostatic spinning</li> <li>Potential for improving mechanical properties of CPs with non-conductive parts</li> <li>Composites often offering other advantages</li> <li>Increased solubility of CPs through the addition of blends, making them suitable for a wide range applications</li> <li>Combining the advantages of both CPs and blended polymers</li> <li>Fast and versatile preparation process</li> </ul>		PANI nanofiber, PVDF/PANI/MWCNTs, and PANI/PU composite nanofiber	16, 19–27
	<ul style="list-style-type: none"> <li>Reduced usage of CPs</li> <li>Preparation of various CPs by removing the template or not according to the demand</li> <li>Enhanced mechanical properties of CPs through templates</li> <li>Feasibility of incorporating additional functionalities through templates, such as drug loading</li> </ul>		PANI, PPY, and PEDOT nanofibers/nanotubes doped with other substances	3, 11, 16, 28–32
	<ul style="list-style-type: none"> <li>Fast and versatile preparation process</li> <li>Reduced usage of CPs</li> <li>Preparation of various CPs by removing the template or not according to the demand</li> <li>Enhanced mechanical properties of CPs through templates</li> <li>Feasibility of incorporating additional functionalities through templates, such as drug loading</li> </ul>		PANI, PPY, PEDOT, and P3HT nanofibers/nanotubes	29, 33–57
Hard template method	<ul style="list-style-type: none"> <li>Nanotubes and nanowires with controllable length and diameter</li> </ul>	<ul style="list-style-type: none"> <li>Removal of templates requiring post-processing</li> <li>Templates affecting the conductivity of CP blends</li> <li>Large fiber diameters that are difficult to control</li> </ul>	PANI, PPY, and PEDOT fibers/nanotubes, PPY nanorods, PPY-GOD-HQS nanowires, PPY nanopillar arrays, PPY nanotube arrays, and Au-PEDOT-Au PPY-CdS coaxial nanowires composited with CP and other substances	58–86
Soft template method	<ul style="list-style-type: none"> <li>Synthesis of nanotube and nanowire arrays with orientation</li> <li>Relatively fast, simple, and continuous process</li> <li>Simple self-assembly process without additional template and template removal process</li> <li>Smaller diameter CP nanofibers with higher electrical conductivity</li> </ul>	<ul style="list-style-type: none"> <li>The quantity of the prepared nanostructures limited by the size of the template</li> <li>Limited in large-scale nanostructure preparation</li> <li>Poor control of fiber morphology preparation, size, and orientation</li> <li>More complex processes</li> <li>Difficult to prepare nanofibers longer than 10 microns in length</li> <li>Uniform for fiber structure</li> <li>Limited fiber length</li> </ul>	PEDOT, PANI, and PPY fibers/nanotubes/nanorods, and PEDOT nanotube arrays	87–110
Directed electrochemical nanowire assembly	<ul style="list-style-type: none"> <li>Faster growth rates and cheaper, safer synthesis methods for nanostructures</li> <li>No need to connect/deposit electrodes after synthesis</li> </ul>		PEDOT and PPY nanowire	65, 111, 112



Table 1 (continued)

Approach	Advantages	Disadvantages	Structure of CPs	Ref.
Other methods				
Radiation-induced synthesis method	<ul style="list-style-type: none"> <li>Fast and efficient preparation</li> <li>Simple synthesis</li> </ul>	<ul style="list-style-type: none"> <li>Requirement of specific equipment</li> <li>Involvement of radiation safety and protection issues</li> </ul>	P3HT nanospheres	99
Solution spinning	<ul style="list-style-type: none"> <li>Suitable for the synthesis of a wide range of materials</li> <li>High aspect ratio</li> <li>Excellent mechanical properties and electrical conductivity</li> </ul>	<ul style="list-style-type: none"> <li>Slower production speeds</li> <li>Possibility of using poisonous reagents</li> </ul>	PPY nanotubes, and PPY, PANI, and PEDOT nanofibers	113–115
3D printing	<ul style="list-style-type: none"> <li>High resolution with specific methods</li> <li>Customization of materials on demand</li> <li>Customization of inks on demand</li> </ul>	<ul style="list-style-type: none"> <li>Requirement of reprocessing device</li> <li>Extrusion prints at low resolution</li> <li>Presence of post-processing</li> <li>Poor solubility of CPs</li> </ul>	3D microstructure PEDOT:PSS	116–119

into nanofibers by a single-nozzle electrospinning technique. Similarly, PPY was successfully processed into nanofibers with improved properties by doping with sodium dodecylbenzene sulfonate, which enhanced its solubility in chloroform.<sup>122</sup> In addition, experimental evidence confirms a significant enhancement in the electrical conductivity of CP nanofibers compared to bulk CPs (powder or film). For example, PPY nanofibers exhibit approximately two orders of magnitude higher conductivity than PPY film, likely due to the substantial molecular chain alignment achieved during electrospinning.<sup>122</sup>

**2.1.2 Coaxial electrospinning.** Coaxial electrospinning is a fiber manufacturing technique known for its high efficiency, continuity, and tunability, utilizing coaxial nozzles in electrospinning equipment to apply high voltages to polymer solutions or molten polymers, resulting in fiber formation. As shown in Fig. 3(A), the coaxial nozzle is a critical component in coaxial electrospinning, featuring a unique geometry where one capillary is located inside the other. This design allows fluid to be transported through the inner capillary, while the outer capillary pump delivers the solution to be electrospun.<sup>1</sup> Therefore, depending on the location of the CPs, the resulting fibers can be categorized into two types: CP core/other shell and other core/CP shell configurations.

In coaxial electrospinning, depending on the composite material, composite fibers can combine different advantages while being formed quickly and efficiently. However, CPs still face challenges such as low solubility and rigid backbones when electrospun as either the shell or core layer solution, often requiring stabilization by adding dopants or other substances. Because of its good solubility in polar solvents, polyvinylpyrrolidone (PVP) is often chosen as the base polymer for coaxial electrospinning. PPY/PVP composite nanofibers have been successfully prepared by blending PVP and PPY as the core layer solution, with PVP used as the shell layer solution.<sup>21</sup> Moreover, CPs in the shell layer are usually used to ameliorate defects in the core layer fibers. For instance, composite nanofibers were synthesized by co-electrospinning poly(vinylidene fluoride)/polyaniline filled with multi-walled carbon nanotube (PVDF/PANI/MWCNT) blends, where the inner capillary was injected with a polyvinylidenefluoride (PVDF) solution, and the outer capillary was filled with PVDF/PANI/MWCNT blends. The resulting composite nanofibers exhibited superior piezoelectric properties compared to non-conducting pure PVDF nanofibers, due to the addition of CPs in the outer layer.<sup>20</sup> Additionally, through selecting suitable solvents and optimizing electrospinning conditions, the successful preparation of PANI/PU composite nanofibers using coaxial electrospinning has been reported. Polyurethane (PU) is highly elastic and biocompatible, while the conductive PANI enhances sensor sensitivity. The composite fibers combine the advantages of both, creating a pH sensor that is soft, stable and highly sensitive.<sup>19</sup>

Besides, further processing after coaxial electrospinning to remove the core or shell is another approach to obtaining nanostructured CPs.<sup>16,22</sup> For example, coaxial nanofibers with PANI as the core and polymethyl methacrylate (PMMA) as the shell were prepared using coaxial electrospinning, the PMMA





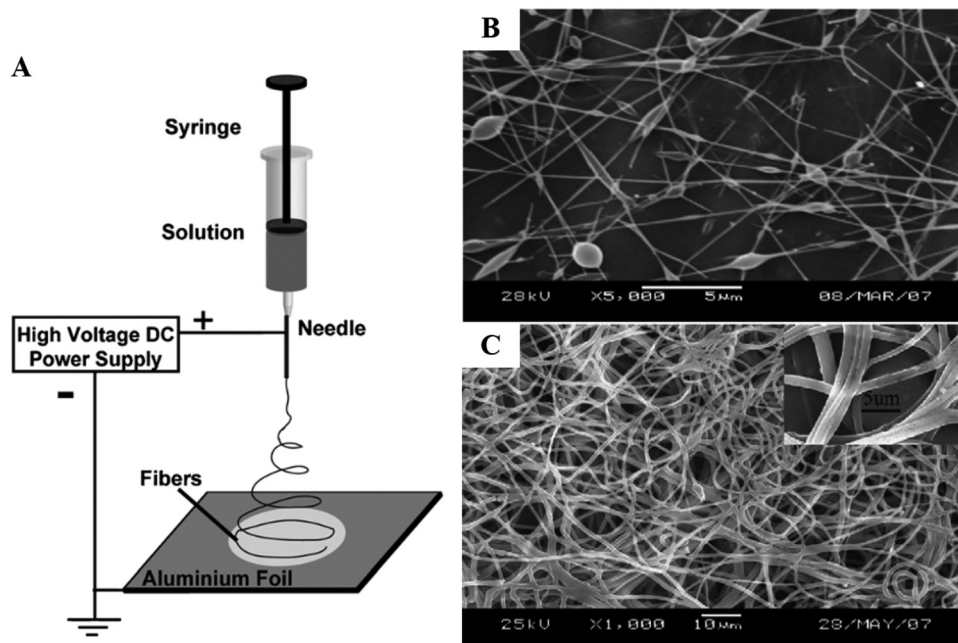


Fig. 2 (A) Schematic of direct electrospinning techniques. SEM images of fibers formed with PANI concentrations of (B) 10.6% and (C) 14.0%, using concentrated sulfuric acid as a dopant. The inset shows the corresponding high-magnification image.<sup>17</sup> Copyright 2008 Elsevier B.V.

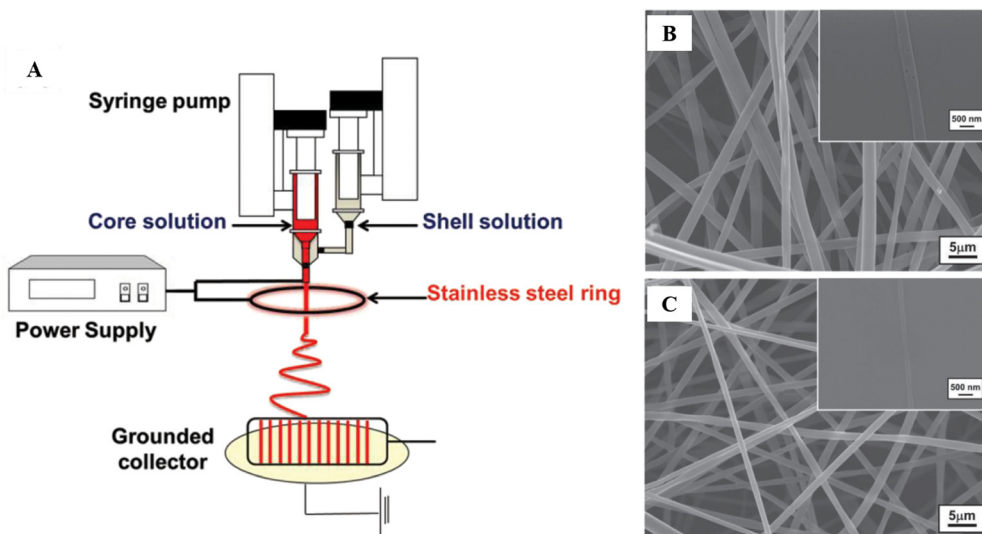


Fig. 3 (A) Schematic of the coaxial electrospinning technique. FE-SEM images of P3HT-PMMA core-shell fibers (B) without and (C) with a secondary electric field. The insets show the core nanofibers (PHTNFs) after removal of the PMMA shell, prepared using coaxial electrospinning with a finer diameter.<sup>23</sup> Copyright 2011 American Chemical Society.

shell layer was later removed by stirring in IPA for one hour, leaving behind oriented pure PANI fibers (Fig. 3(B) and (C)).<sup>23</sup> Coaxial electrospinning significantly enhances the performance of P3HT nanofibers, achieving a field-effect mobility of  $1.92 \times 10^{-1} \text{ cm}^2 \text{ V}^{-1} \text{ s}^{-1}$  and an on/off ratio of  $4.45 \times 10^4$ , representing a three-orders-of-magnitude improvement over conventional methods. This improvement is likely due to the slower solidification of CPs in the inner layer, resulting in a more stable elongation process, higher molecular orientation, and enhanced charge-carrier mobility.<sup>23</sup>

**2.1.3 Co-electrospinning with other polymers.** Co-electrospinning of CPs with other copolymers is a common method, as the incorporation of other soluble polymers makes CPs easier to process during electrospinning. The typical approach involves blending CPs and polymers in the same solution system, which is then shaped in one step by electrostatic spinning.<sup>32,120</sup> To illustrate, Moutsatsou *et al.*<sup>11</sup> successfully prepared CSA/PEO-doped PANI conductive fibers by mixing camphorosulfonic acid (CSA), PANI and PEO in a chloroform solution as the precursor solution, followed by standard single-needle electrospinning. This research



further explored the factors affecting the morphology of electrospun nanofibers. Ultimately, ambient humidity was identified as the most critical factor for successful fiber preparation, and it was demonstrated that both voltage and flow rate significantly affect the diameter of the nanofibers. Moreover, blending with other polymers allows for better processing of CPs, while the addition of polymers with specific properties provides CP/copolymer composite fibers with advantages in areas such as drug release, tissue regeneration, and conductive scaffolds.<sup>14,30</sup> Composite nanofibers were prepared by electrospinning PPY blended with sericin proteins (Fig. 4(A)), which showed more matched tensile properties (Fig. 4(B)) and more matched Young's modulus (Fig. 4(C)) compared to PPY nanofibers alone and can be used to enhance the functionality of engineered myocardial tissues.<sup>28,120</sup> However, the insulating polymers typically blended in these composites often result in decreased conductivity. To address this issue, a study applied the concept of secondary doping to electrospinning, using *m*-cresol as a secondary dopant. This approach, alongside co-electrospinning using CSA, PEO, and PANI, produced oriented nanofibers with a conductivity of  $1.73 \text{ S cm}^{-1}$ , which is two orders of magnitude higher than the average conductivity observed in similar studies.<sup>3</sup>

In addition, Feng *et al.*<sup>42</sup> spun an ethylene dioxythiophene (EDOT) monomer and poly(lactide-*co*-glycolide) (PLGA) co-mixture through a Taylor cone, subsequently exposing it to an oxidation catalyst for polymerization. The template was then removed in chloroform, resulting in PEDOT nanotubes with electrical conductivity and orientation (Fig. 4(D)). The approach highlighted the potential advantages of PEDOT nanotubes in applications such as nerve regeneration or drug delivery.

**2.1.4 Electrospun fibers as templates.** Direct electrospinning of CPs is straightforward but faces limitations, including a narrow application range, large nanofiber diameters, and the use of toxic solvents. Co-electrospinning introduces other substances that can partially mitigate these issues, though it may also compromise the conductivity of the CPs. In contrast, the template method allows for the creation of nanostructured CPs while integrating with other processes, resulting in composite nanofibers that retain the inherent high electrical conductivity of CPs while enhancing their physical/chemical properties.<sup>2</sup> In the template method, electrospun nanofibers serve as stable templates for the subsequent growth of various CPs, which allows the resulting CPs to adopt the internal morphology of the fiber exterior, leading to a larger specific surface area and

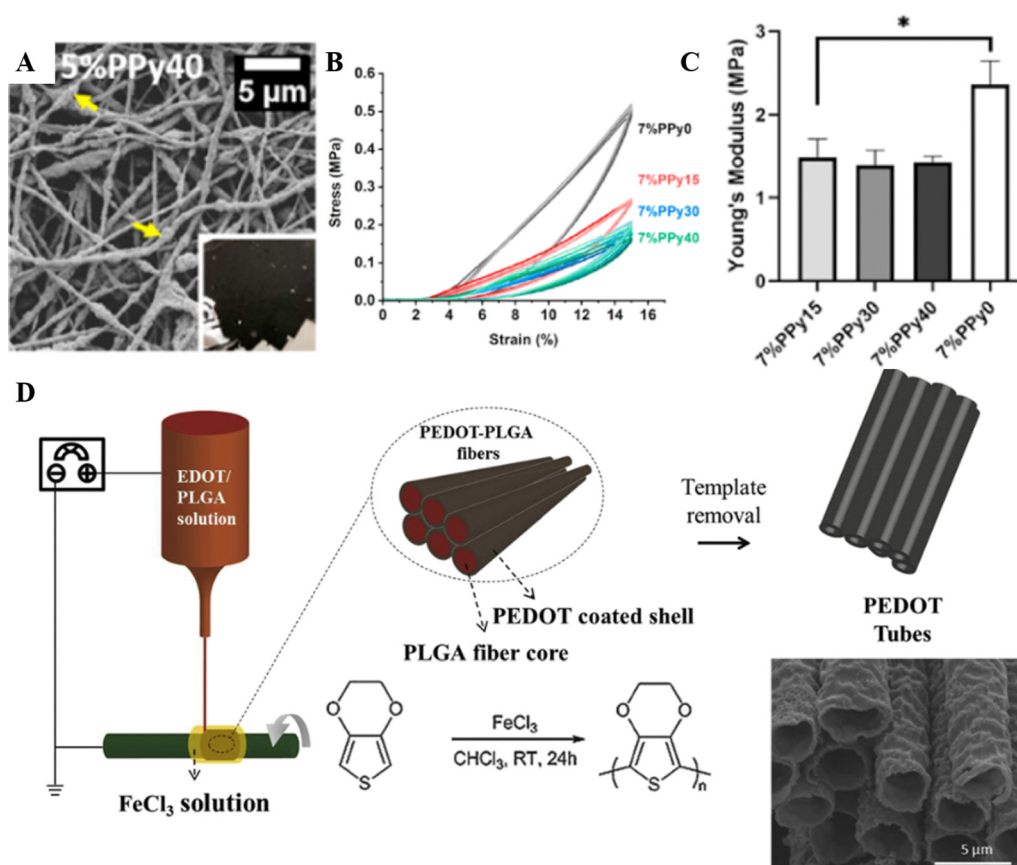


**Fig. 4** (A) SEM images of nanofibers obtained by electrospinning PPY blended with SF. (B) Cyclic tensile stress–strain curves and (C) Young's modulus of ES mats with different PPY ratios, showing that increased SF content improves tensile properties and reduces the Young's modulus of the fibers.<sup>28</sup> Copyright 2021 Elsevier Ltd. (D) Polymerization of PEDOT monomers co-blended with PLGA, exposed to oxidizing agents to obtain oriented electrospun PEDOT shell/PLGA core microfibers, along with a schematic of the synthesis of PEDOT nanotubes with orientation through chloroform template removal.<sup>42</sup> Copyright 2012 Elsevier Ltd.



offering more reaction sites. It should be noted that the nanofiber template must be removed during or after the polymerization of CPs. Consequently, an ideal nanofiber template should satisfy three key criteria: (1) facile electrospinnability into fibers, (2) structural stability during CP polymerization and inertness to process substances and environment, and (3) facile template removal. The main approaches for CP polymerization on electrospun fiber templates include solution deposition polymerization and gas-phase deposition polymerization.

Typically, the solution deposition polymerization method requires a separate solution system containing CP monomers, oxidants, and doping acids. The CP monomers are usually reactively polymerized on the surface of the nanofibers. Examples include the polymerization of PANI,<sup>38,40,41,49</sup> PPY,<sup>33,47</sup> poly(3-thiophenethanol) (P3TE),<sup>37</sup> PEDOT,<sup>42</sup> and others. Miao *et al.*<sup>40</sup> immersed electrospun PAN fibers in a solution containing aniline monomer, FeCl<sub>3</sub> and HCl for 12 h. After subsequent washing and drying, nanofibers with a composite shell-core structure of PANI and PAN were obtained. Another approach involves hydrophobic treatment of electrospun PMMA nanofibers, which enables PANI to specifically adsorb on the surface, forming a composite core-shell structure.<sup>38</sup> The nanofiber templates were then removed in chloroform, resulting in a PANI nanotube structure. Similarly, Dong *et al.*<sup>49</sup> prepared composite PANI/PLA structures using poly(lactic acid) (PLA) nanofibers as templates, and interestingly employed the thermal degradation method to remove the templates, yielding PANI nanotubes. This method of template removal is advantageous due to its ease of handling and environmentally friendly nature, but it also imposes stricter requirements on both CPs and nanofiber templates. The CPs must remain stable at the template decomposition temperature without experiencing cross-linking or structural damage. Additionally, selected nanofiber templates must not only adhere to the earlier mentioned three criteria but also decompose at a temperature lower than the threshold of the CPs, posing certain limitations on the choice of CPs and templates.

Electrochemical *in situ* polymerization is frequently used in solution deposition polymerization methods, where reactive sites loaded with nanofiber templates are immersed in an electrodeposition solution containing CP monomers. These monomers deposit on the surface and continue to grow on the surface of nanofiber templates over time, leading to the formation of one-dimensional electrically conductive compounds with nanotubular channels.<sup>34–36,39,44,45</sup> For instance, Abidian *et al.* utilized PLGA<sup>35</sup> and poly-L-lactide (PLLA)<sup>36,39,44</sup> nanofibers as templates to modify PPY or PEDOT on the surfaces *via* constant current deposition. After removing the templates with chloroform or dichloromethane, nanotubular structures of the CPs were obtained.<sup>36</sup> The CPs with nanotunnel structures significantly reduced the impedance of micro-electrodes by approximately two orders of magnitude and increased the charge transfer capability by about three orders of magnitude, as demonstrated through corresponding surface electrochemical studies.<sup>39,45</sup> Meanwhile, Abidian and colleagues investigated the conditions for electrodepositing CPs to

achieve nanotube structures. They found that a deposition current density of 1.44 C cm<sup>-2</sup> resulted in the most stable nanotube formations, yielding lower impedance (19.5 ± 2.1 kΩ for PPY nanotubes and 2.5 ± 1.4 kΩ for PEDOT nanotubes at 1000 Hz) and higher charge capacity densities (184 ± 5.3 mC cm<sup>-2</sup> for PPY and 392 ± 6.2 mC cm<sup>-2</sup> for PEDOT at 1000 Hz).<sup>36</sup> Both nanotubes exhibited superior properties compared to the corresponding CP films, with PEDOT demonstrating particularly enhanced electrochemical properties.<sup>39</sup> Moreover, Chen *et al.*<sup>46</sup> utilized poly(ε-caprolactone) (PCL) nanofibers as templates for electrodeposition to obtain CPs with nano-tunneling structures, incorporating carbon nanotubes (CNTs) as the counter-ions (Fig. 5(A)). Their studies, including ultrasonic and CV tests, confirmed that the PEDOT-CNT nano-tunneling structures reduced impedance and exhibited greater stability than PEDOT-PSS counterparts, with coating adhesion improved by a factor of 1.5. Compared to conventional solution deposition and vapor phase deposition methods, a key advantage of electrochemical *in situ* polymerization is its localized formation of CPs in conductive regions, enhancing control while allowing other areas of the nanofibers to potentially enhance biocompatibility, drug loading and release capabilities. Specially, Abidian and Martin designed a PLLA nanofiber template loaded with dexamethasone, which was wrapped in an alginate hydrogel scaffold.<sup>44</sup> They employed electrochemical *in situ* polymerization to deposit a conducting polymer, forming nanotubes that utilize dexamethasone as an anti-inflammatory agent while simultaneously reducing impedance, opening up more possibilities for neural interfaces in biomedicine.

In the vapor phase deposition method, the first requirement is that the nanofibers prepared by electrospinning must contain an oxidant capable of polymerizing the CP monomers. The CP monomers are then oxidatively polymerized on the surface of the nanofibers in an atmosphere saturated with the monomers (Fig. 5(B)–(D)).<sup>42,52</sup> Subsequently, CP nanotubes are obtained through a depyrolysis process (Fig. 5(E) and (F)).<sup>54,56</sup> Using polyacrylonitrile (PAN) nanofibers as a template for vapor phase deposition of gold-doped PANI core-shell structures, Wang *et al.*<sup>52</sup> demonstrated that the doping of gold nanoparticles, combined with the nanostructures of CPs, resulted in enhanced field-effect mobility. This approach offers a promising method for preparing high-performance organic field-effect transistor materials. Furthermore, Laforgue *et al.*<sup>56</sup> developed a method combining electrospinning and gas phase polymerization to produce PEDOT nanofibers. Initially, PEDOT nanotubes were electrospun with PVP and a small amount of pyridine. Subsequently, EDOT monomers were polymerized by vapor deposition onto oxidant-containing nanofibers. After removing excess reactants and products with methanol and drying, the PEDOT nanotubes were shrunk to nanofibers with minimal interporosity. The CP nanofibers produced by this method exhibited very high electrical conductivity and have potential for applications in flexible electronics.

All of the above examples involve polymer nanofibers as templates. However, there are methods that use electrospun inorganic materials, such as TiO<sub>2</sub>,<sup>43,48,51,54</sup> Mn<sub>2</sub>O<sub>3</sub>,<sup>50</sup> and V<sub>2</sub>O<sub>5</sub><sup>55</sup>





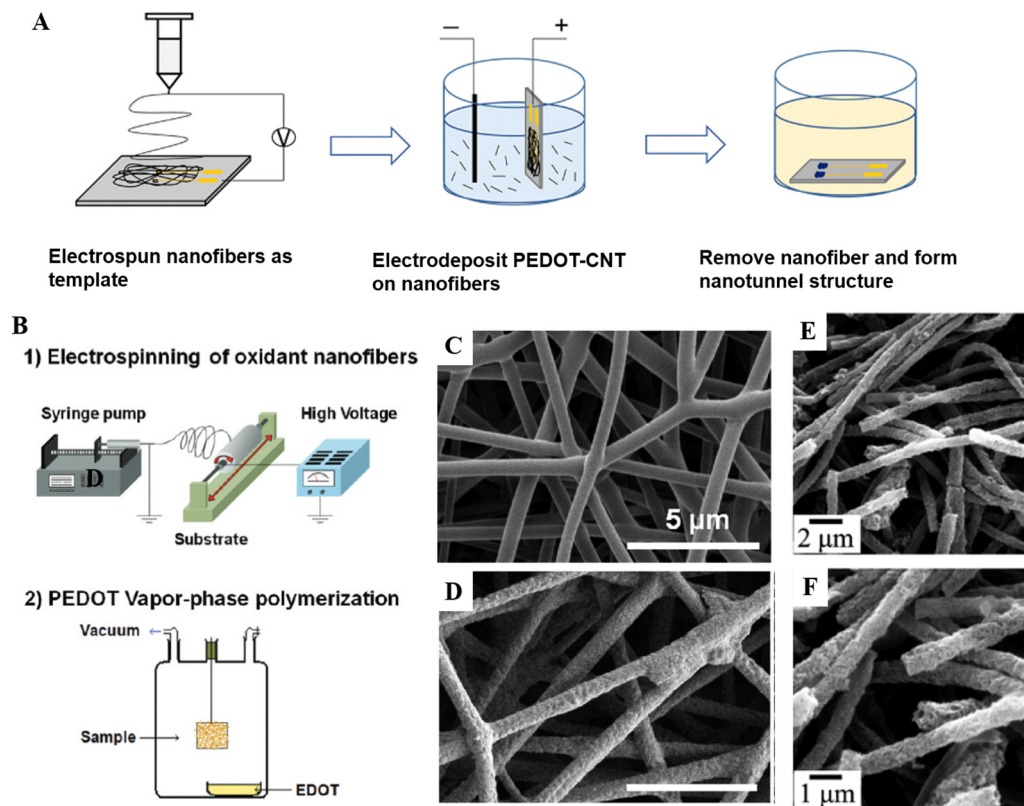


**Fig. 5** (A) Schematic diagram of the formation of a nanotunnel structure following the removal of the template by *in situ* electropolymerization of CPs using electrospun fiber as a template.<sup>46</sup> Copyright 2020 American Chemical Society. (B) Schematic diagram of the CP shell layer prepared using electrospun fiber as a template and then *via* gas-phase deposition. SEM images of nanofibers (C) before and (D) after gas-phase polymerization, using electrospun fiber as a template for the polymerization of CP *via* gas-phase deposition.<sup>56</sup> Copyright 2010 American Chemical Society. (E) and (F) SEM images of PANI nanotubes after removal of the nanofiber template.<sup>41</sup> Copyright 2013 American Chemical Society.

as nanofiber templates for subsequent deposition polymerization. Both solution and vapor phase polymerization can be applied in these cases, offering alternative approaches to preparing CP-based nanostructures. In an ingenious approach, Li *et al.*<sup>50</sup> used  $\text{Mn}_2\text{O}_3$  fibers as templates, where the nanofibers not only serve as the template but also act as oxidants in the polymerization reaction. Ultimately, the  $\text{Mn}_2\text{O}_3$  templates were able to be spontaneously removed to obtain pure PANI nanotubes. It was also reported that PEDOT was successfully modified on the surface of nanofibers by first electrospinning  $\text{TiO}_2$ , followed by calcination and vapor phase deposition techniques. This method demonstrated that the PEDOT nanotubes produced had excellent photocatalytic properties, opening up new possibilities for the development of related sensors.<sup>54</sup> Furthermore, one team successfully prepared 'bamboo-like' PPY nanotubes using  $\text{V}_2\text{O}_5$  nanofibers as sacrificial templates through vapor phase deposition.<sup>55</sup> This approach offers an advantage over the conventional nanofiber template methods, as the  $\text{V}_2\text{O}_5$  nanofibers gradually change color from light yellow to dark green during the reaction, with a corresponding reduction in mass, eliminating the need for a separate template removal step.

Electrospinning technology offers several strategies for the preparation of CP nanofibers, but each method has advantages

and disadvantages (Table 1). Overall, these methods face key challenges: heavy reliance on toxic solvents, prominent contradiction between conductivity and processability, complex processes (*e.g.*, multistep deposition, template removal), insufficient systematic research on molecular chain arrangement and long-term stability under hygrothermal/mechanical stress, and limited practical application adaptability, with most results still confined to laboratory validation.

## 2.2 Hard template method

The hard template method is a synthetic approach for producing nanostructured CPs that employs rigid template materials.<sup>1,5,75,123</sup> Frequently used templates encompass prefabricated nanofibers,<sup>36,41,46</sup> porous materials (*e.g.*, anodic aluminum oxide (AAO) and particle track-etched membranes (PTMs)),<sup>57,63,66,74,82,85,124</sup> and biopolymeric or biological templates, including chitosan<sup>59</sup> and viruses.<sup>58,84</sup> The specific operational process of the hard template method involves several key steps: template making, template filling, precursor transformation, and template removal. First, appropriate materials are selected to create a template with the desired structure. The template's surface may then undergo chemical or physical treatment to modify its properties. Next, the precursor solution or gas of the material to be synthesized is introduced into the template, which features a nanostructure





that ensures uniform distribution of the precursor. Following this, the precursor materials are converted into the desired nanomaterials through methods such as heat treatment or chemical reactions, which may involve crystal growth or nanoparticle formation. Finally, the template is removed using methods like dissolution or ablation, resulting in a replica or antipattern of the synthesized nanomaterial (Fig. 6).

CP nanowires with controllable lengths and diameters were first successfully synthesized by Martin<sup>74</sup> at the end of the last century *via* nanoporous membranes. The key advantage of this method is its ability to easily produce controllable, highly orientated nanostructures, with the diameter of the resulting CP nanowires reaching single-digit nanometer level. Other porous materials frequently used as hard templates for synthesizing CPs with nanostructures include polycarbonate films, AAO, and PTM.<sup>85</sup> Callegri *et al.*<sup>66,85</sup> used porous templates combined with electrochemical polymerization to synthesize size-controllable, multisegmented metal/conjugated polymer nanowires by simply altering the electrodeposition solution. This approach opens avenues for creating CP composites with other substances, particularly magnetic metals, enhancing their potential for fundamental research in organic spintronics and applications in electronic devices. Similarly, a mixture of pyrrole, glucose oxidase (GOD) and 8-hydroxyquinoline-5-sulfonic acid (HQS) was electropolymerized within an AAO template using its nanopore-like structure, leading to the preparation of PPY-GOD-HQS nanowires with enhanced power density.<sup>78</sup> Another research team started by preparing PU porous elastomers with a sponge-like structure using sugar templates, followed by *in situ* polymerization of pyrrole within the sponge structure of the PU templates.<sup>80</sup> This method produced a uniform porous template while reducing costs, providing a solid foundation for forming the unique nanostructures of the subsequent CPs.

In addition to commonly used porous materials, other substances are frequently reported as hard templates.<sup>1,61,125</sup> The use of nanofibers as templates, followed by template filling through various methods such as solution deposition or vapor phase deposition to obtain CPs with nanostructures,<sup>35,36,41,44,60</sup> has already been discussed in detail in earlier sections and will not be reiterated here. Ryu *et al.*<sup>125</sup> proposed an Au-ZnO-Au-PEDOT electrode, which demonstrated the lowest impedance, phase angle, and the largest charge storage capacity compared to controls, making it ideal for applications requiring flexibility and high performance, such as in the brain-computer interfaces. The preparation process involves etching specific areas on the Au electrode surface, growing ZnO nanowires ( $\sim 3.5 \mu\text{m}$ ) using a hydrothermal method, sputtering Cr/Au onto the nanowires, and finally electrochemically polymerizing PEDOT on the modified nanowires to obtain PEDOT with nanostructures. Moreover, researchers have explored using the pores within metal-organic frameworks (MOFs) as templates for growing CPs, replicating the inner surface morphology of the pores. The templates were subsequently removed by successive acid-base treatments to yield PEDOT nanowires. This method significantly reduced the Young's modulus while maintaining electrical conductivity comparable to bulk PEDOT, suggesting that

these flexible nanomaterials have potential for applications in sensing and energy conversion.<sup>69</sup> In addition to inorganic substances, biomolecular templates like viruses and self-assembled protein complexes offer promising platforms for constructing nanomaterials with unique functionalities. These templates have the advantage of allowing genetic manipulation and chemically specific biocouplings at near-atomic precision.<sup>83,84</sup> For instance, Gan *et al.*<sup>59</sup> successfully formed conductive PPY nanorods by *in situ* polymerization within a hydrogel network, using a chitosan framework as a molecular template. This process endowed the conductive hydrogel with excellent electrical conductivity, mechanical properties, and biocompatibility. Moreover, natural tobacco mosaic virus (TMV) particles possess a unique tubular structure and distinctive physicochemical properties, making them ideal templates for forming one-dimensional nanomaterials through internal or external deposition. In one study, TMV was used as a template to prepare homogeneous PANI/TiO<sub>2</sub> hybridized nanofibers, demonstrating potential for use in composite membranes capable of sensing liquefied petroleum gas.<sup>84</sup> Additionally, DNA templates offer a unique advantage in the design and synthesis of multifunctional composite CPs due to their special self-recognition and self-assembly properties.<sup>81</sup> The growth mechanism involves CP nucleates and growth at the binding sites on the DNA, which gradually transforms into smooth CP nanowires with excellent electrical conductivity under the condition of limiting the amount of template material per unit length.<sup>62</sup>

The hard template method has several disadvantages, including the tedious preparation of polymers or templates and the challenges associated with subsequent template post-processing.<sup>1,68,123</sup> In response to these limitations, a "self-sacrificial template method" has been proposed. These self-sacrificial templates not only provide a hard surface for polymer growth and polymerization but also often involve the action of oxidizing agents.<sup>55,118</sup> Additionally, the templates can degrade through water-soluble degradation<sup>86</sup> or thermal degradation.<sup>49</sup> For instance, Dai *et al.*<sup>83</sup> utilized FeCl<sub>3</sub>-methyl orange self-degrading fibers as templates to create hollow PPY nanotube structures. They capitalized on the stability of methyl orange fibers in acidic environments and their solubility in neutral water, successfully removing the methyl orange template in water after the PPY had polymerized on its surface.

In addition to the conventional hard template methods discussed earlier, alternative approaches such as photolithographic patterning techniques<sup>67</sup> and high aspect ratio nanochannel array glass films<sup>71</sup> have emerged as promising methods for synthesizing high-density CP nanostructures. These nanolithography-assisted templates have significant potential in various applications, including semiconductor materials, energy, and sensors, making them of great interest in the development of advanced technologies.<sup>5</sup>

The hard template method enables the controlled preparation of nanostructured CPs through rigid templates. This approach offers the advantages of precise structure and high orientation, exemplified by CP nanowires with single nanometer diameters. Improved methods, such as self-sacrificial templates and



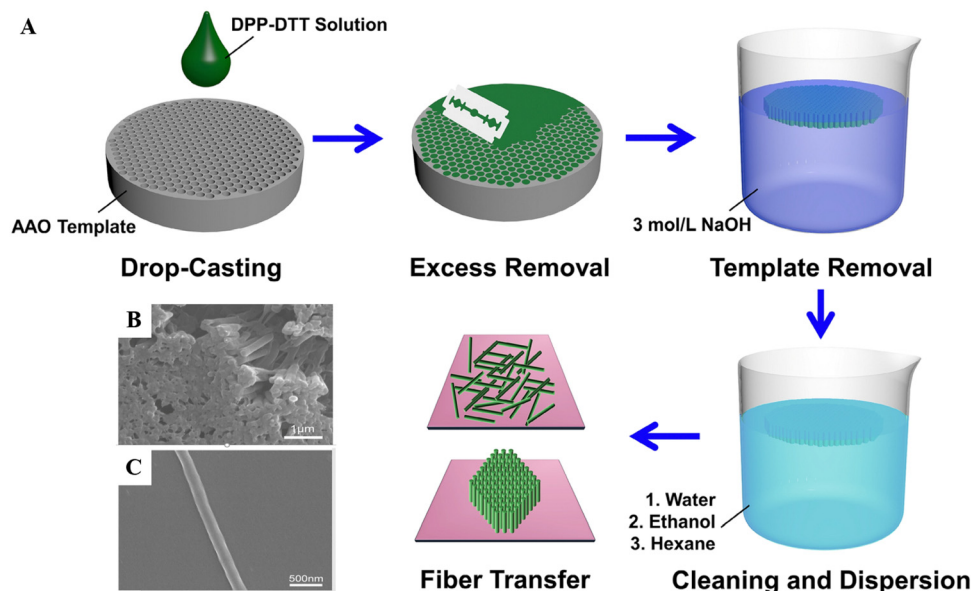


Fig. 6 (A) Schematic of the preparation of CP nanowires using AAO templates. SEM images of tightly stacked polymer nanowires standing on (B) a substrate and (C) a single polymer nanowire.<sup>82</sup> Copyright 2023 Donghua University, Shanghai, China.

photolithography, have partially addressed the challenge of template removal and expanded the application scenarios, including flexible electronics and sensing. However, the preparation process remains complex and costly. Template removal may damage material properties, for instance, chemical corrosion can destroy the structure. Additionally, the stability of biological templates and the feasibility of large-scale production are still questionable. The high equipment threshold of new methods, such as photolithography, also restricts their industrial applications. Future efforts should focus on optimizing the process, reducing costs, and developing milder and more environmentally friendly template removal strategies.

### 2.3 Soft template or solution self-assembly method

The soft template method synthesizes nanostructured CPs through a self-assembly process driven by intermolecular forces, including hydrogen bonding, van der Waals forces,  $\pi$ - $\pi$  stacking, dispersion forces, and metal coordination.<sup>123</sup> A key advantage over hard template methods is the simplified self-assembly, eliminating the need for template removal. Furthermore, the soft template method can produce CP nanofibers with smaller diameters, enhancing electrical conductivity. However, limitations include reduced control over fiber morphology, size, and orientation, and difficulty in producing nanofibers exceeding 10  $\mu\text{m}$  in length.<sup>4,10</sup> Depending on the type of template used, soft template methods can be roughly categorized as template-free or micellar polymerization,<sup>94,110,126,127</sup> interfacial polymerization,<sup>109</sup> and reversed-phase emulsion polymerization.<sup>128,129</sup>

The template-free method is a straightforward self-assembly approach that eliminates the need for an external template, allowing for the control of the final product's morphology through the manipulation of synthesis conditions. This method has successfully yielded one-dimensional structures of CPs, such

as nanofibers and nanotubes (Fig. 7(A)). Factors influencing the diameter and morphology of the self-assembled nanofibers include the structure of the monomer, dopant, and oxidant, as well as the concentrations of the reactants, the molar ratios among components, and the temperature, time and mode of the reaction.<sup>105,126</sup> For example, Wan transformed PANI hollow microspheres into one-dimensional nanotubes (Fig. 7(C)) by simply varying the polymerization temperature or adjusting the molar ratio of the dopant to the monomer.<sup>110</sup> In template-free methods, micelles typically serve as the primary template, guiding the self-assembly of the CPs. Micelles formed by carboxylic acids have been proposed as soft templates in the preparation of PANI nanotubes through self-assembly.<sup>105</sup> In this approach, various acids act as dopants, with hydrogen bonding between the polymer chains and hydroxyl groups facilitating the self-assembly of the nanotubes. This highlights that the template-free method is primarily influenced by two key factors: the micelles and the competitive reaction between the micelles and the monomers. By optimizing the parameters, stable soft templates can be achieved while rebalancing the competition between micelles and monomers, leading to the formation of better-shaped CPs in an optimal equilibrium state. Additionally, CP nanofibers can be prepared using the interiors of micelles as templates.<sup>90</sup> In this approach, sodium dodecyl sulfate (SDS), an anionic surfactant, is utilized. Following the formation of rod-like micelles, the EDOT monomer is drawn into the micelles due to interactions with hydrophobic groups and subsequently undergoes oxidative polymerization. While this method yields nanofibers (Fig. 7(B)) with a small diameter, their length is typically limited to a few micrometers. Notably, the nanofibers synthesized in this manner exhibit higher electrical conductivity compared to those produced through conventional methods. Another approach involves synthesizing nano-PEDOT in an



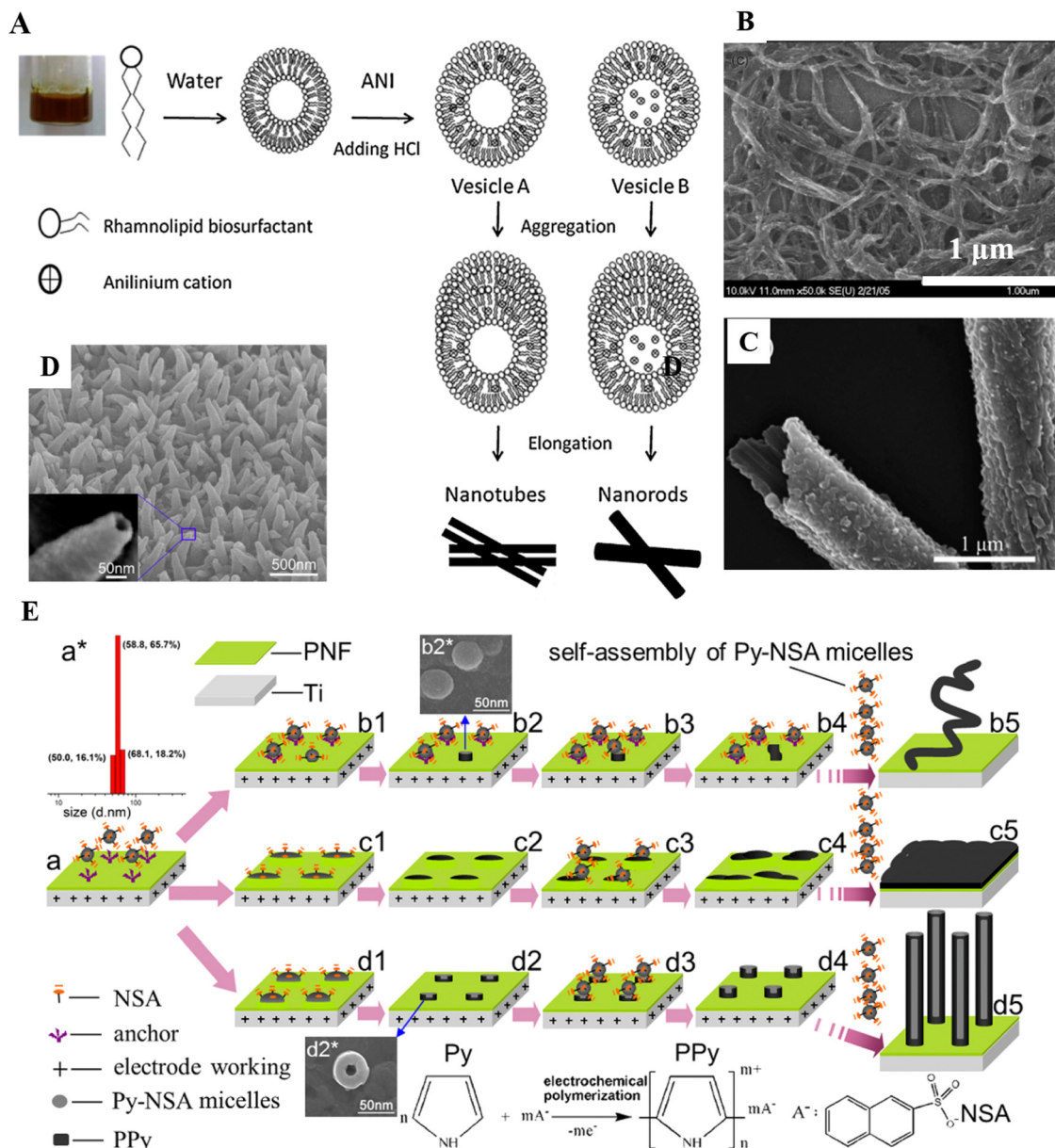


**Fig. 7** (A) Schematic illustrating the formation of micelles by self-assembly of dopants, acting as soft templates, where CPs polymerize externally to form nanotubes. Additionally, the formation of nanowires occurs by dopant protection, with the polymerization taking place inside the micelles.<sup>104</sup> Copyright 2010 Elsevier B.V. SEM images of (B) PEDOT nanowires<sup>90</sup> and (C) CP nanotubes<sup>110</sup> synthesized by the soft template method. Copyright 2006 WILEY-VCH Verlag GmbH & Co. KGaA, Weinheim; Copyright 2015 Royal Society of Chemistry. (D) SEM image of oriented nanowire arrays. (E) Formation of oriented nanowire arrays by polymerization on substrates. Polymerization, protected by the dopant, predominantly occurs at the tips of nanowires to form these arrays.<sup>103</sup> Copyright 2014 American Chemical Society.

aqueous solution of poly(4-sodium styrenesulfonate) (PSS), where PSS functions as both a counterion and a surfactant.<sup>94</sup> Besides, ordered one-dimensional CP arrays facilitate shorter ion transport paths, often resulting in enhanced electrical properties. These arrays can be achieved through the self-assembly of conducting PPy nanotubes, which is driven by the creation of an isotropic two-dimensional space formed by specific “anchoring points” between the pyrrole micelles and the conducting substrate (Fig. 7(D) and (E)).<sup>103</sup> This mechanism promotes the formation of organized CP nanotube arrays.

Interfacial polymerization is a method in which different monomers or reagents are dissolved in two mutually insoluble phases, allowing the polymerization reaction to occur at their interface. This method offers the advantage of producing uniform PANI nanofibers with diameters of approximately 50 nm without requiring additional templates or functional dopants.<sup>95</sup> However, SEM characterization revealed that PANI tended to form dendritic structures, which may result in insufficient lengths of the nanofibers. To mitigate the secondary growth of primary PANI nanoparticles during interfacial polymerization,



Yu and colleagues successfully synthesized PANI nanorods with uniform dimensions through gentle stirring. The modified material, enhanced with PVP, demonstrated a high dielectric constant and low dielectric.<sup>130</sup> In the field of electrical conductivity, flexible tubular highly crystalline nano-needles offer fast response times on the millisecond scale. To enhance crystallinity, Nuraje and colleagues developed an interfacial polymerization method using low concentrations of monomer and oxidant, successfully preparing single-crystalline PANI and PPY nano-needles, which also demonstrated general applicability to other CPs.<sup>131</sup> It is worth mentioning that interfacial polymerization occurs at the interface of two immiscible phases, which implies that in addition to liquid/liquid interfacial polymerization, gas/liquid interfacial polymerization is also a viable method for synthesizing nanostructured CPs.<sup>132</sup>

Reversed-phase emulsion polymerization, which involves the aggregation of surfactant molecules containing a nanoscale aqueous phase within the oil phase, is frequently used to prepare nanoconductive polymers. For example, Jiang *et al.* first reported the preparation of PPY nanotubes using this method by adding sodium bis(2-ethylhexyl) succinate sulfonate to hexane to form anticlusters.<sup>128</sup> The polymerization was completed by adding FeCl<sub>3</sub> and CP monomers to this mixed system. The addition of an oxidant (FeCl<sub>3</sub>) reduces the “second micelle concentration” and increases the ionic concentration of the solvent, which promotes the formation of rod-like micelles. AOT, an amphiphilic surfactant with two hydrophobic tail groups and a hydrophilic head group, efficiently forms antimicelles in the oil phase due to its large hydrophobic tail.<sup>133,134</sup> Additionally, the anionic polar end group of AOT can extract metal cations from the solution into the antimicelles, thereby creating a rod template with oxide ions on the surface.<sup>135</sup> Meanwhile, the use of other surfactants in the preparation of CPs has also been reported. For instance, PANI nanofibers with a dendritic structure (about 60–90 nm in diameter) were synthesized by the chemical oxidative polymerization of aniline in a surfactant gel formed in a mixture of cetyltrimethylammonium chloride (C16TMA), acetic acid, aniline, and water.<sup>129</sup>

Soft template methods synthesize nanostructured CPs by self-assembly *via* intermolecular forces, avoiding the hard template removal step and allowing the preparation of small-diameter (enhanced conductivity) but length-limited (<10 μm) nanofibers. Template-free methods achieve morphology control by modulating reaction conditions but rely on micellar competitive equilibrium with questionable reproducibility. The interfacial polymerization generates homogeneous nanofibers (~50 nm) but is prone to branching and requires additional optimization (*e.g.*, stirring, additives) to inhibit secondary growth. The reversed-phase emulsion polymerization uses surfactants to form a template for the antimicellulose micelles, but relies on specific reagents (*e.g.*, AOT) and is limited in terms of cost and environmental friendliness. Despite the significant increase in conductivity, the lack of morphology control, difficulty in scale-up, and length limitations constrain their application in long-range conductive or precision devices. In the future, it is necessary to balance the self-assembly kinetics and

template stability, and develop more universal and controllable synthesis strategies.

## 2.4 Directed electrochemical nanowire assembly

Directional electrochemical nanowire assembly is a technique that uses electrochemical methods to assemble nanowires in specific directions and positions, as shown in Fig. 8(A). In this process, an alternating electric field is applied to a salt solution, inducing a reduction reaction of the solute, and nanowires are grown at the desired location and orientation based on the electrode configuration. Compared to vapor phase growth, this method offers faster growth rates and is more cost-effective and safer.<sup>111</sup> As shown in Fig. 8(B), CP nanowires around 400 nm were successfully grown between two electrodes.<sup>136</sup>

CP nanowires with fast growth rates have been successfully prepared by a directed electrochemical nanowire self-assembly technique. However, despite its success in the laboratory, this technique still faces challenges of complex electrode configurations and control of nanowire homogeneity in large-scale production, limiting its potential for industrial transformation. In addition, current applications are mainly focused on specific solutes (*e.g.*, CP), and the generalizability to multimaterials or composite structures has not yet been verified, making the technology scalability questionable. Meanwhile, the interfacial bonding strength and electrochemical corrosion tolerance of nanowires have not been sufficiently investigated, which may lead to their structural degradation in dynamic working environments. Therefore, despite the breakthrough of this method in directional growth efficiency, its robustness in complex scenarios still needs to be further verified, and a complete reliability evaluation system is urgently needed.

## 2.5 Other methods

In addition to the common synthesis methods mentioned above, various specialized templates and techniques for preparing nanostructured CPs have also been reported in the literature. Examples include the evaporation-induced self-assembly method (EISA), low-polymer template method, and wet spinning radiation-induced synthesis method,<sup>98</sup> and 3D printing, among others.

A newly synthesized pyrrole-containing compound, *N'*1, *N'*6-bis(3-(1-pyrrolyl)propanoyl) hexanedihydrazide, has been reported to form CP nanowires by EISA and pyrrole-ring-stacking-driven self-assembly, followed by chemical polymerization of pyrrole groups located on the surface of the micro-rods.<sup>88</sup> Furthermore, Lu *et al.*<sup>100</sup> proposed synthesizing nanostructured PEDOT using PVA as a template, where hydrogen bonding between hydroxyl groups on PVA and ether oxygen on PEDOT served as the driving force for the formation of nanostructures. Additionally, Liang and colleagues<sup>101</sup> reported self-assembled lithocholic acid nanotubes *via* weak interactions, where pyrrole adsorbed onto lithocholic acid and polymerized to form nanotube hydrogels. After lyophilization, the resulting PPY nanotubes had a nanotube network and hierarchical porous structure, giving them excellent electrical conductivity





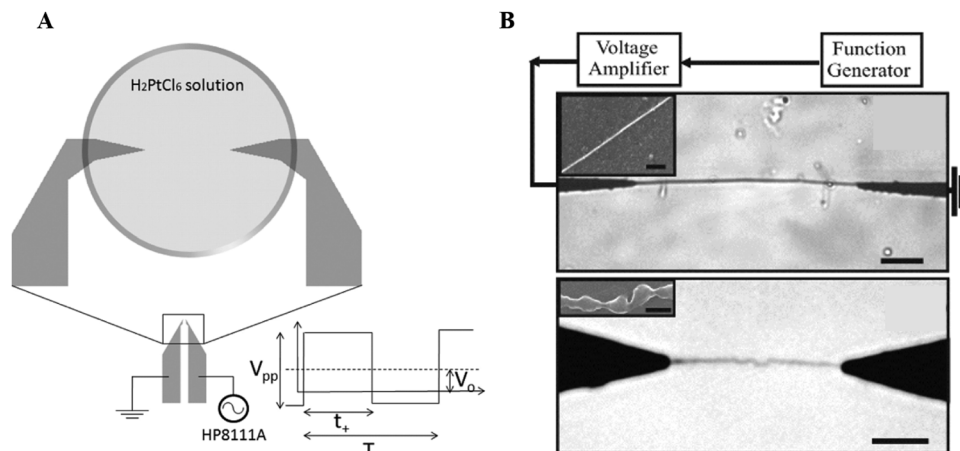


Fig. 8 (A) Schematic of the device for directed electrochemical assembly.<sup>111</sup> Copyright 2011 American Chemical Society. (B) Nanowires synthesized by directed electrochemical assembly.<sup>136</sup> Copyright 2009 IOP Publishing.

and strain resistance, with potential applications in tissue scaffolds and strain sensors.

Wet spinning is a process where a fiber-forming polymer is dissolved in a suitable solvent to create a spinning solution with the required viscosity and spinnability. This solution is then extruded through a nozzle into a coagulation bath. As the solvent diffuses into the bath and the coagulant infiltrates the solution, the polymer reaches a critical concentration and precipitates, forming fibers.<sup>113–119</sup> For instance, Li *et al.*<sup>113</sup> prepared PEDOT:PSS microfibers by wet spinning technology and enhanced their electrical conductivity and mechanical properties by incorporating ionic liquids, offering a new idea for the development of high-performance, multi-functional wearable smart fabrics.

3D printing of CPs is an emerging method for fabricating nanostructured CPs using techniques such as extrusion printing, photopolymerization printing, and direct ink writing.<sup>116–118</sup> This approach enables customizable geometries and functionalities, making it ideal for flexible electronics and biosensors. However, extrusion printing suffers from low resolution due to nozzle size and layer-by-layer deposition, while photopolymerization printing is limited by the strong light absorption of CPs, restricting light penetration and photosensitizer activation.<sup>118,119</sup> Recently, Zhou *et al.*<sup>117</sup> developed a highly efficient HAT (homolytic aromatic substitution) catalyst that enables rapid photopolymerization *via* a dual HAT reaction, allowing the construction of 3D conductive micro-nanostructures with sub-micron resolution and programmability, effectively overcoming these challenges.

The synthesis methods of nanostructured CPs are increasingly diversified. Self-assembly techniques have enabled high-precision structural tuning by virtue of intermolecular forces to successfully prepare nano-CPs, while 3D printing has shown great potential in the fabrication of micro- and nanostructures and flexible electronic devices by virtue of its high degree-of-freedom customization capability. However, most of the current methods remain in the laboratory stage, and industrialization faces many challenges, such as high costs, complex processes (*e.g.*, EISA), and dependence on precision equipment

(*e.g.*, 3D printing). Self-assembled structures suffer from insufficient mechanical stability, performance degradation due to template or solvent residues, and lack of biocompatibility validation for biomedical applications, while 3D printing is limited by the nozzle size, which constrains its technological translation. In the future, green processes need to be developed through interdisciplinary collaboration, such as the use of recyclable templates and environmentally friendly solvents, optimization of the resolution and material compatibility of 3D printing, and enhancement of long-term testing of material properties in complex environments, in order to promote nanostructured CPs from the laboratory to real-world applications in mass production.

### 3. Nanostructured CPs for biomedical applications

Nanostructures impart unique properties to CPs, such as enhanced conductivity that enables efficient electron transfer, and reduced resistance that minimizes energy loss and improves conversion efficiency. The increased specific surface area provided by nanostructures offers more active sites for improved electrochemical reaction rates and better contact with other materials. Additionally, the small size of nanostructures allows CPs to be formed into thin films, nanowires, and nanoparticles with tunable shapes and sizes to meet various application needs. These advantages make nanostructured CPs highly versatile for use in electronics, energy, sensors, optoelectronics, and biomedicine. In addition to their shape tunability and excellent electrical conductivity, CPs used in biomedical fields must possess good biocompatibility, stability, and tunable electrochemical properties. The precise configuration of CP nanostructures can promote cell adhesion and growth while better mimicking and monitoring biophysiological electrical signal transduction, making them highly suitable for applications in tissue engineering, biosensing, and bioelectronic devices. In this section, we focus on biomedicine and



briefly introduce the recent applications of nanostructured CPs in drug delivery, neuroelectrodes and interfaces, neural regeneration, and biosensors.

### 3.1 Drug delivery and targeted therapy

Recent decades have witnessed a surge in drug delivery systems utilizing materials such as nanoparticles, graphene, and carbon materials, where drug release is often triggered by factors such as thermal transitions, pH changes, or electrical stimulation.<sup>137,138</sup> Electrically stimulated drug release is a highly competitive method for treating acute or chronic diseases, as it allows for target therapy and controlled drug delivery in response to external stimuli.<sup>139</sup> CPs are frequently selected as carriers for electrostimulated drug delivery due to their excellent electrical properties akin to metals, outstanding mechanical stability, ease of processing, and ability to bind or release charged ionic molecules on demand based on varying redox states.

Typically, model drugs in electrostimulation therapy serve dual roles: they act as therapeutic agents, such as anti-inflammatories or repair substances, and as dopant ions that enhance the stability of the CPs' nanostructure. For example, Esrafilzade *et al.*<sup>137</sup> prepared PEDOT:PSS fibers by wet spinning and used them as a template for the electropolymerization of a PPY shell layer. In the synthesis of PPY, ciprofloxacin hydrochloride served both as a model drug and as a dopant, with the release of oppositely charged ciprofloxacin hydrochloride observed during the reduction reaction. Similarly, the direct electrochemical polymerization of the chemotherapeutic drug methotrexate (MTX) as a dopant for PPY has been investigated.<sup>140</sup> By modifying with cetylpyridine, the nanostructure quality of both MTX and PPY improved, as the hydrophobic chains of the surfactant adhered to the hydrophobic PPY, while additional aromatic interactions between the pyridine salt head and the MTX ring significantly enhanced MTX loading. This offers insights for further improving the CP nanostructures and increasing electrically controlled drug loading.

Nanostructured CPs offer significant advantages over conventional CP powder in drug delivery and targeted therapy applications. Their unique self-supporting, three-dimensional flexible architecture renders them ideal for both *in vitro* and *in vivo* biomimetic applications. Furthermore, the higher surface-to-volume ratios inherent to nanostructured materials enable enhanced drug encapsulation rates.<sup>139</sup> Crucially, nanostructured CPs exhibit superior electrochemical activity and lower electrochemical impedance, resulting in significantly improved drug release efficiencies upon electrical stimulation. For example, Lee *et al.*<sup>141</sup> utilized an anodic aluminium oxide film as a sacrificial template and electrochemically deposited PPY with biotin as a dopant, resulting in an improved encapsulation rate when DOX was attached to biotin. Moreover, Ru *et al.*<sup>142</sup> developed an innovative drug release system based on a network of adenosine triphosphate (ATP) and PPY nanowires, where ATP served as both a crystal-directed agent, guiding the formation of the CP nanowire network, and as a model drug released during electrical stimulation. The study demonstrated that the CP nanowire network had higher

electrochemical activity, lower electrochemical impedance, and significantly improved electrorelease efficiency. The system achieved 90% ATP release after 45 h of electrostimulation, compared to about 53% release from a PPY nanomembrane.

The drug loading and release mechanism in the CPs varies based on the specific drug molecules used. As previously mentioned, small anionic drugs can be directly co-doped into the CPs as dopants, with drug release regulated by the application of an electric potential (Fig. 9(A)). In contrast, the current mainstream anionic doping method involves special steps to enhance doping efficiency and overall performance. As shown in Fig. 9(B), the process begins with the synthesis of more stable CPs using alternative anionic dopants. Next, a reduction potential is applied to expel these dopants, allowing the desired drug to be co-oxidized with the CPs as a secondary dopant.<sup>139</sup> On the other hand, there are relatively few examples of cationic drugs being loaded and released.<sup>143,144</sup> As illustrated in Fig. 9(C), the cationic drug is first loaded onto the anion-doped CP skeleton, followed by oxidation of the polymer skeleton through electron injection to release the drug.

Beyond ionic doping, drugs can also be absorbed or encapsulated into nanostructures.<sup>139,145</sup> This method typically involves using other polymers to load the drug into the polymer fibers, which are then coated with CPs. During electrical stimulation, the CPs undergo a redox reaction, causing slight contraction that facilitates drug release from the fibers. These examples highlight the need to develop CPs in conjunction with other polymers to achieve enhanced performance and versatility. One of the challenges in smart and controlled healthcare is the precise and controlled release of drugs. Abidian *et al.*<sup>45</sup> developed a method to grow CP nanotubes on nanofiber templates for caller-controlled drug release. Three key factors influence drug release in this study. First, as PLGA nanofibers undergo hydrolysis, the encapsulated drug is released. Second, during the reduction process, electrons are injected into the polymer chains. To maintain charge neutrality, negatively charged counterions migrate to the solution, leading to nanotube contractions due to electrostatic forces. The contraction alters the oxidation state of the PEDOT encapsulation layer, generating a force on the fiber template that squeezes the inner nanofibers, thereby impacting drug transport and kinetics. Lastly, during an electronically controlled switching cycle, the CP overlay may open or crack, allowing for the natural release of surface-bound drugs from areas of high to low concentration (Fig. 9(D) and (E)).<sup>5,45</sup> The cumulative drug release profiles at five discrete time intervals, as depicted in Fig. 9(F), corroborate the efficacy of the PEDOT-PLGA shell-nucleus construct in facilitating drug release upon exposure to specific voltage stimulation.

Recent research has highlighted PEDOT:PSS nanofibers for electrically triggered drug release. Conductive fibers for controlled painkiller delivery are fabricated using core-shell microfluidic spinning. Incorporating conductive fillers introduces micro-cracks within the fibers, which respond to electrical stimulation, enhancing drug diffusion and release.<sup>146</sup> This on-demand release minimizes drug waste and side effects, improving patient compliance and enabling smart healthcare integration. Electrical stimulation optimizes drug release kinetics,



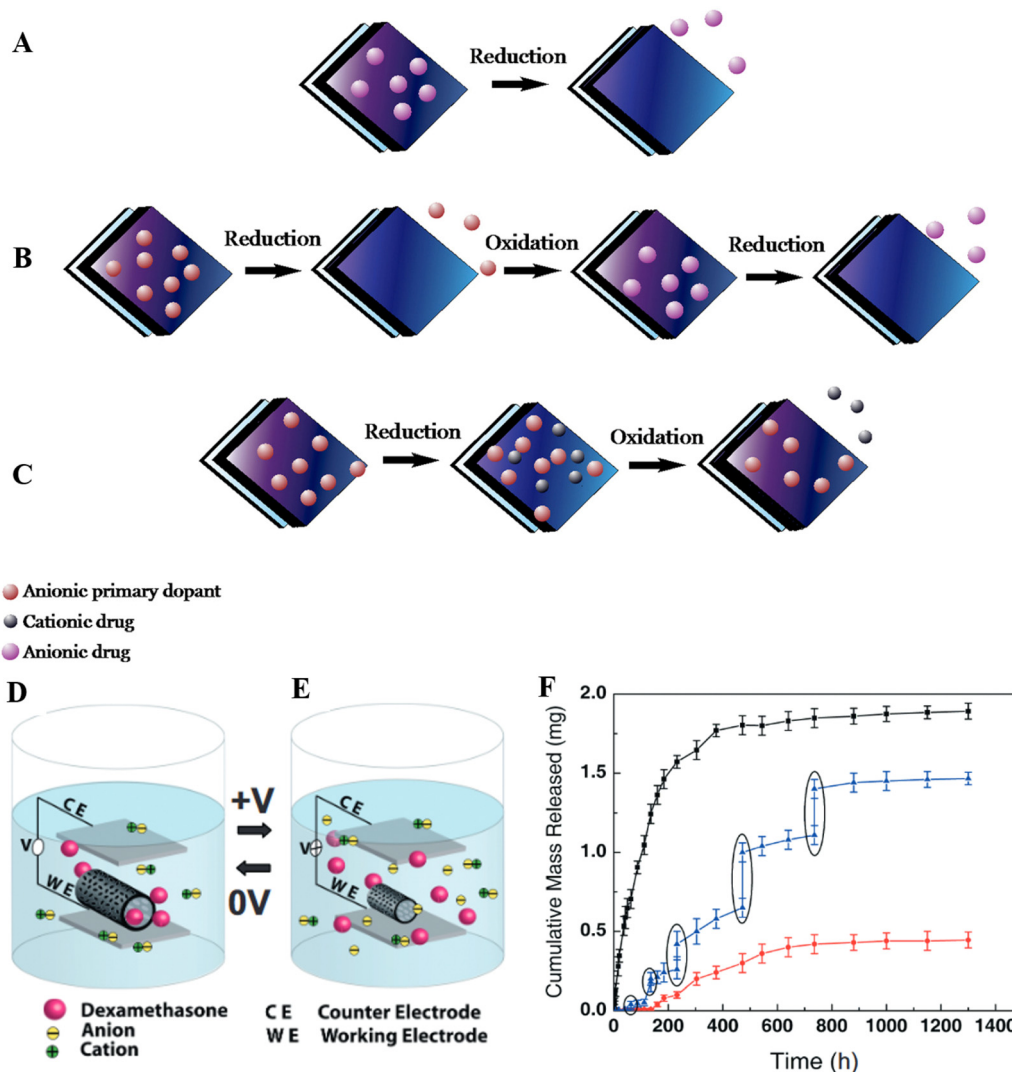


Fig. 9 Schematic representation of the three drug loading and release processes: (A) direct doping with anionic drugs and reductive release from the CP matrix; (B) doping with a primary dopant followed by anionic drug substitution and reductive release from the CP matrix; and (C) oxidative release from the CP matrix based on the adsorption of cationic drugs onto the CP skeleton.<sup>139</sup> Copyright 2019 Elsevier B.V. Schematic representation of the drug release from CP nanotubes by contraction: (D) electrically neutral conditions of CP nanotubes; (E) the application of voltage results in contraction or expansion of the CP nanotubes, with contraction facilitating drug efflux from the ends of the tubes. (F) Cumulative release profiles of the drug from: PLGA nanofibers (black squares), PEDOT-PLGA shell-core structure without electrical stimulation (red circles), and electrically stimulated PEDOT-PLGA shell-core structure at 5 specific time points (blue triangles).<sup>45</sup> Copyright 2009 WILEY-VCH Verlag GmbH & Co. KGaA, Weinheim.

showing promise for wearable devices and telemedicine, including remote monitoring.<sup>147,148</sup>

The development of smart drug delivery systems has received much attention, with the core objective of improving the precision and therapeutic efficacy of drug release. Nanostructured CPs, with their excellent electrical conductivity and special nanostructures, can be electrically stimulated to achieve a certain degree of precise controlled drug release.<sup>5</sup> Electrochemically deposited CP nanotubes can release drugs in response to an external voltage.<sup>45</sup> However, this single stimulus mode restricts the precision of drug delivery. Recently, an injectable hydrogel that combines the electrically responsive properties of CP and the pH sensitivity of hydrogels was developed to achieve precise on-off pulsed drug release.<sup>149,150</sup>

In the future, it is expected that the conductive properties of nanostructured CPs can be further improved by optimizing the preparation process, thereby enhancing the precision of electrically controlled drug release. In addition, through surface modification or compounding with other materials, nanostructured CPs can be integrated with more functions, which will promote the development of drug delivery systems towards intelligence and precision.

Despite the promising advancements, several challenges and limitations hinder the widespread application of CPs in drug delivery. A primary concern is the long-term biocompatibility and potential toxicity of CPs and their degradation products *in vivo*. While many studies demonstrate short-term biocompatibility, comprehensive long-term studies are crucial

to assess any adverse effects. The inherent brittleness of some CPs, particularly in their doped state, can lead to mechanical failure and inconsistent drug release, especially in dynamic physiological environments.<sup>137,151</sup> Furthermore, the precise control over drug release kinetics remains a challenge. Factors such as the CP's morphology, doping level, and the interaction between the drug and the polymer matrix can significantly influence release profiles, requiring careful optimization for each specific drug and application. The scalability of manufacturing processes for nanostructured CPs, while maintaining consistent properties and drug loading, also presents a significant hurdle for clinical translation. Finally, achieving targeted delivery to specific tissues or cells, beyond the site of implantation or administration, often requires further functionalization of the CPs with targeting moieties, adding complexity to the system.

### 3.2 Neuroelectrodes and interfaces

Neuroelectrodes function as interfaces that collect and convert electrophysiological signals at the cellular level into electronic signals for analysis and decoding. The electrochemical impedance of the electrode, along with the charge injection capacity, are also important indicators for assessing the performance of neuroelectrodes in research. In recent years, neuroelectrodes have decreased in size, achieving higher spatial resolution. However, the reduction in the electrode's working area significantly increases electrochemical impedance, which negatively impacts the detection quality of subsequent electrophysiological signals. Therefore, obtaining lower impedance while minimizing electrode size has become a key research focus.

In particular, CPs represented by PPY and PEDOT are increasingly used to modify neuroelectrode surfaces, as they have been shown to substantially reduce impedance while remaining compatible with living cells.<sup>152</sup> Nanostructured CPs offer distinct advantages over thin-film alternatives in terms of electrochemistry, stability, and other characteristics. Abidian and colleagues prepared a series of CP nanotube-structured neural microelectrodes using electrospinning fiber templates.<sup>39,44,45</sup> Specifically, the surface modification of neuroelectrodes with dexamethasone-loaded biodegradable nanofibers, which are subsequently coated with alginate hydrogel, is followed by the electrochemical polymerization of PEDOT onto the electrode surface. This process results in the formation of CP nanotubes that encapsulate the nanofibers and integrate within the hydrogel scaffolds (Fig. 10(A)–(D)). Electrochemical tests demonstrated that CP nanotubes significantly improve the electrochemical performance of microelectrodes, exhibiting lower impedance (Fig. 10(E)), higher charge transfer capability and charge density (CCD) (Fig. 10(F)) for the same deposited charge density ( $1.44 \text{ C cm}^{-2}$ ) compared to bare electrodes, PPY nanolayers, and PEDOT nanolayers.<sup>39,44</sup> The intrinsic gap ratio of CPs contributes to a relatively high specific surface area. When applied to neuroelectrodes, the one-dimensional structure increases the electrochemical surface area, effectively reducing impedance and improving the signal-to-noise ratio.<sup>123</sup> Notably, PPY and PEDOT nanotubes demonstrate stronger adhesion properties compared to their film counterparts, likely due to

their more porous and softer structure, which reduces internal strain during actuation. The subsequent work confirmed this hypothesis by developing PEDOT–CNT nanotunneling structures on the surface of neuroelectrodes to achieve high-fidelity neural signals, using CNT as a doping ion. Following a 20-minute ultrasonication process, thin sections treated with the PEDOT–CNT nano-tunnel exhibited enhanced adhesion, as depicted in Fig. 10(G). Moreover, it was observed that the electrode integrated with the PEDOT–CNT nano-tunnel demonstrated a notably higher amplitude of nerve signals and a reduced noise amplitude, as illustrated in Fig. 10(H). The introduction of CNTs not only enhanced the stability of the nanostructures but also improved the adhesion of the coatings by up to 1.5 times.<sup>46</sup>

In contrast to conventional metallic electrodes, CPs have emerged as a compelling class of materials for neuroelectrode applications due to their unique combination of electrical conductivity, biocompatibility, flexibility, and tunable properties.<sup>1,45</sup> Beyond metals, other materials such as carbon-based nanomaterials (e.g., graphene, carbon nanotubes) have also been explored for neural interfaces. Carbon nanomaterials offer high conductivity and large surface area, but often require complex processing and face challenges in long-term biocompatibility.<sup>153</sup> Notably, a recent study has showcased the potential of CPs by developing a transparent, patternable, and stretchable solid electrode based on modulating the ratio of block polymer to PEDOT:PSS. This innovative approach, leveraging optimized component ratios, achieves remarkable electrical and mechanical performance,<sup>153</sup> and even demonstrates actuation capabilities comparable to traditional non-solid electrodes in dielectric elastomer actuators. Such advancements underscore the promise of CPs in delivering high-performance solutions for the next generation of flexible bioelectronic interfaces and smart materials integration.

Additionally, the field of neuroelectrodes has rapidly evolved from rigid structures to stretchable and flexible devices, enabling the integration of CPs with soft materials such as elastomers<sup>153,154</sup> and hydrogels.<sup>155</sup> These combinations enhance processability and biocompatibility. For instance, PEDOT:PSS microfibers dispersed in a polyurethane matrix create a flexible conductive network, which can be precisely patterned using laser techniques to fabricate high-performance electrode arrays.<sup>153</sup> Additionally, nanostructured CPs improve electrical conductivity and electrochemical properties while encapsulation in elastomers minimizes PSS release, enhancing both biocompatibility and stability.<sup>155</sup>

The ideal neuroelectrode interface must balance low impedance, excellent biocompatibility, and long-term stability.<sup>8</sup> Nanostructured CPs have emerged as a promising solution due to their ability to dramatically reduce interfacial impedance and enhance electrochemical performance; for instance, electrochemically deposited PEDOT nanotubes can lower electrode impedance by approximately two orders of magnitude.<sup>36,45</sup> However, maintaining the stability of these nanostructures over extended periods remains a significant challenge, as redox reactions on the electrode surface and micromovements within tissues can lead to delamination or detachment of the nanostructured CP coatings, which are often prepared by





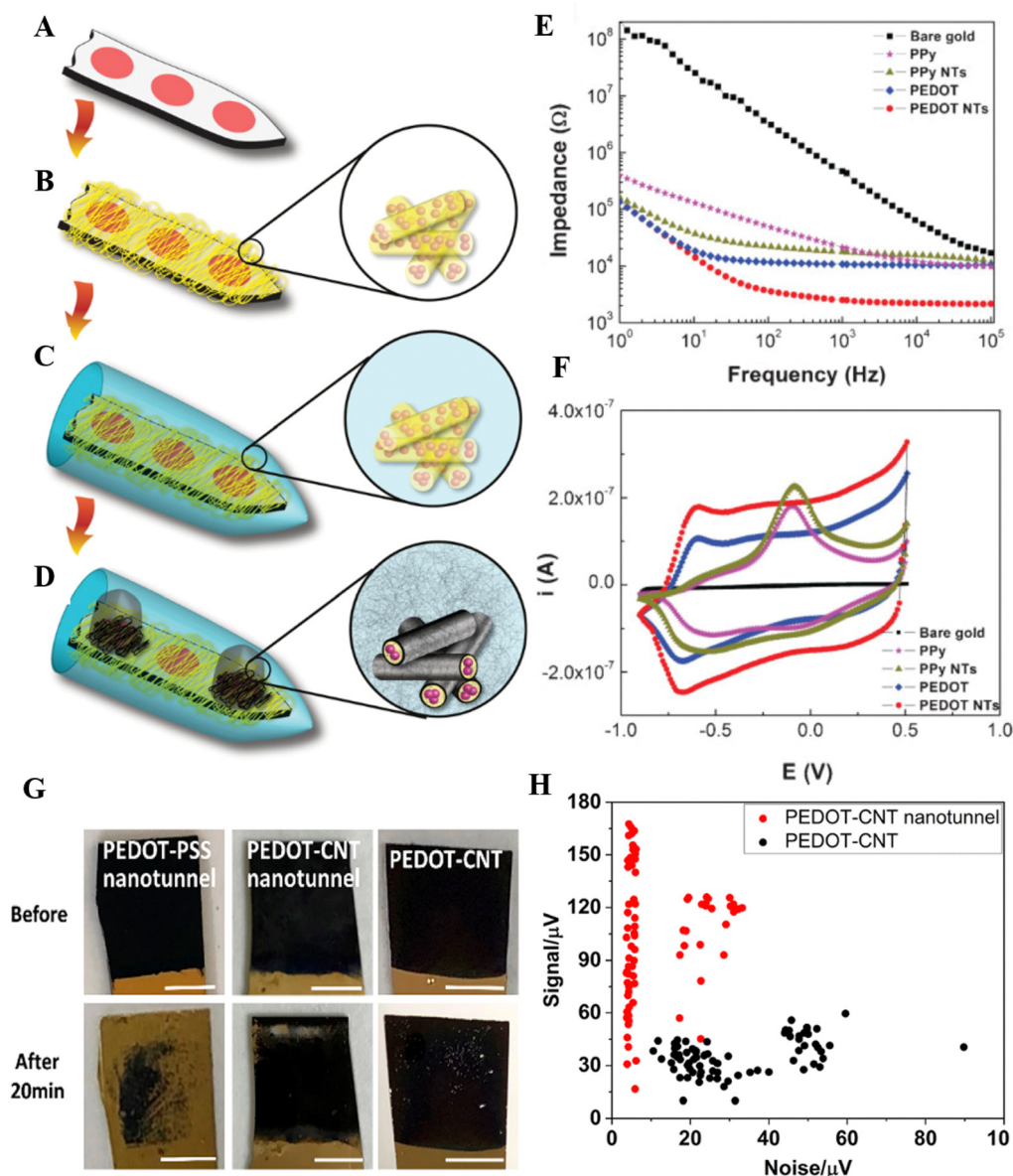


**Fig. 10** (A)–(D) Modification of dexamethasone-loaded biodegradable nanofibers on the surface of the neuroelectrode, followed by alginate hydrogel coating, and electrochemical polymerization of PEDOT on the electrode, with the CP nanotubes surrounding the nanofibers and within the hydrogel scaffolds.<sup>45</sup> Copyright 2009 WILEY-VCH Verlag GmbH & Co. KGaA, Weinheim. (E) Bode plots of the electrochemical impedance spectra in the frequency range of  $1\text{--}10^5$  Hz, showing that CP nanotubes have significantly lower impedance than CP films. (F) Cyclic voltammograms of modified CP films and CP nanotubes, with potential scanned from 0.9 to 0.5 V at a scan rate of  $100\text{ mV s}^{-1}$ , indicating that CP nanotubes have higher CCD than the nanofilms.<sup>36</sup> Copyright 2010 WILEY-VCH Verlag GmbH & Co. KGaA, Weinheim. (G) Optical images of PEDOT-PSS nano-tunnel coatings, PEDOT-CNT nano-tunnel coatings, and PEDOT-CNT coatings before (top) and after (bottom) sonication for 20 min. Scale bar: 5 mm. (H) Scatter plots of signal amplitude (peak-to-peak) and noise level recorded at PEDOT-CNT nanotunneling and PEDOT-CNT-coated sites, demonstrating that nanotunneling structure-modified microelectrodes have a higher signal-to-noise ratio.<sup>46</sup> Copyright 2020 American Chemical Society.

conventional methods such as electrochemical deposition or template methods.<sup>156,157</sup> Traditional strategies have focused on chemically anchoring and cross-linking the coatings to strengthen their adhesion to the electrode interface,<sup>156</sup> while more recent innovations have involved embedding nanostructured CPs into polymer networks to achieve mechanical interlocking between conductive nanomaterials and polymer surfaces, thereby significantly enhancing the robustness of the

interface between electrodes and conductive layers.<sup>157</sup> Moving forward, maintaining both the stability of nanostructured CPs and low interfacial impedance over long-term use is crucial, and efforts should be directed toward developing and refining new preparation methods to meet the stringent requirements of neuroelectrode interfaces.

In the realm of neuroelectrodes and interfaces, nanostructured CPs are widely used due to their exceptional electrical



conductivity. The integration of nanostructured CPs with other flexible materials has accelerated the development of flexible wearables even more. However, this field still faces serious challenges. Nanostructured CPs are prone to coating delamination due to redox reactions or tissue micromotion in long-term dynamic physiological environments, and the existing strategies for enhancing adhesion (chemical anchoring, mechanical interlocking) lack long-term stability validation. Second, the existing preparation processes are too complex (*e.g.*, electrospinning template method, laser patterning) for large-scale production. In addition, multimodal electrodes are one of the development trends, but multifunctional integration may introduce signal interference (*e.g.*, drug release affecting the electrochemical environment). In the future, self-repairing or degradable CPs need to be developed to enhance durability and safety, a standardized long-term *in vivo* evaluation system needs to be established, and the design needs to be optimized through interdisciplinary synergies (*e.g.*, microfluidics, AI) to solve the problem of conflicting functionalities, and to promote the translation of neuroelectrodes from laboratory innovations to reliable clinical applications.

### 3.3 Nerve regeneration

Nervous tissue comprises multiple, well-arranged bundles of nerves, with information transfer typically occurring *via* electrical signaling at synapses between neurons. Consequently, when reconstructing injured nerves, it is often desirable to mimic natural nerve tissue as closely as possible, ideally achieving precise control over axonal growth direction and structural polarization.<sup>123,158</sup> The beneficial effects of electrical stimulation on nerve regeneration are well documented, notably in promoting neuronal differentiation, enhancing neural protrusion growth, and guiding directed axon growth.<sup>12,159,160</sup> CPs are promising candidates for neural tissue engineering due to their excellent electrical conductivity and biocompatibility. However, their relatively poor mechanical properties and solubility limitations restrict their applications.<sup>12,14,161</sup> Thus, CPs are often combined with other materials to improve processability, and it has been demonstrated that one-dimensional structures of CPs, such as nanofibers and nanotubes, offer superior electrochemical properties and better support for cell adhesion and growth.<sup>161</sup>

Notably, electrospinning has become a prevalent method for producing oriented composite nanofibers. Yang and colleagues utilized PCL/PANI nanofibers to promote the differentiation of pheochromocytoma (PC12-L) cells into neuron-like cells.<sup>162</sup> The incorporation of PANI improved both the biocompatibility and electrical conductivity of PCL, facilitating cell adhesion and promoting their functional potential. A key highlight of this work is the rapid preparation of CP composites with an oriented structure using 304 stainless steel mesh as a fluid collector. The combination of highly ordered nanofibers and electrical conductivity effectively supports the differentiation of PC12-L into neuron-like cells, presenting a promising approach for nerve regeneration.

In peripheral nerve tissue engineering, Schwann cells (SCs) play a critical role. These cells synthesize and secrete neurotrophic

factors and extracellular matrix molecules that actively guide and promote axonal regeneration. Remyelination by SCs is essential for effective nerve conduction in regenerating peripheral axons.<sup>12,160</sup> Because obtaining a sufficient quantity of SCs is challenging, research has increasingly focused on inducing the differentiation of other stem cells into SCs. For example, studies have shown that orderly arranged conductive nanofibers can induce bone marrow mesenchymal stem cells (BMSCs) to differentiate into Schwann-like cells (Fig. 11(C)). Given the synergistic relationship between SCs and conductive axons, the conductive properties of these nanofibers are likely a primary factor influencing stem cell differentiation into SCs.<sup>163,164</sup> Furthermore, in peripheral nerve regeneration applications, combining CPs with natural polymers and immunomodulatory drugs synergistically promotes nerve regeneration, enhances functional recovery, and prevents muscle atrophy.<sup>165</sup> This approach represents a promising strategy for treating peripheral nerve injuries.

Nerve conduits are an effective approach for treating short-distance nerve injuries. Two common fabrication methods are 3D printing and electrospinning. 3D printing is advantageous for producing nerve conduits with precise geometries that mimic the native biological environment. For example, Farzan *et al.* fabricated nerve conduits with precise geometries using 3D printing, demonstrating excellent electrical conductivity, mechanical properties, and biocompatibility.<sup>166</sup> Electrospinning, on the other hand, can produce oriented CP nanofibers. Studies have shown that scaffolds with both conductivity and fiber orientation are crucial for aligning neurons and facilitating electrical signal transmission.<sup>123,158,159</sup> Ordered CP nanofibers promote SC differentiation and enhance the extension and alignment of dorsal root ganglia neurons, effectively acting as a “bridge” for nerve defect repair. As shown in Fig. 11(A) and (B), the damaged nerve stumps are connected to both ends of the nerve conduit, allowing axons to grow along the conduit, gradually regenerating from the proximal to the distal end. Tuj1 immunofluorescence in dorsal root segments, cultured on ordered composite nanofiber scaffolds (Fig. 11(D)) for three days *in vitro*, is depicted in Fig. 11(E). The PPY/PDA/PLLA group exhibited improved neurite alignment and length, as shown in Fig. 11(F). Quantitative analysis confirmed these observations, revealing longer neurites with good alignment in the PPY/PDA/PLLA. A bionic piezoelectrically oriented PPY/PDA/PLLA composite nanofiber nerve conduit was successfully developed, demonstrating that these three materials synergistically provide excellent electrical conductivity and cytocompatibility. The combination restored the piezoelectric effect diminished by the addition of polydopamine (PDA) and facilitated the regeneration and functional repair of the sciatic nerve.<sup>159</sup>

Beyond electrical stimulation, effective neural repair also depends on the electrical conductivity of the substrate and the inherent function of the nerve cells. Therefore, combining 3D bioprinting and electrospinning technologies to create PPY/SF composite scaffolds with fine micropatterned internal structures offers significant advantages.<sup>12</sup> These scaffolds exhibit excellent toughness, conductivity, and stability under electrical





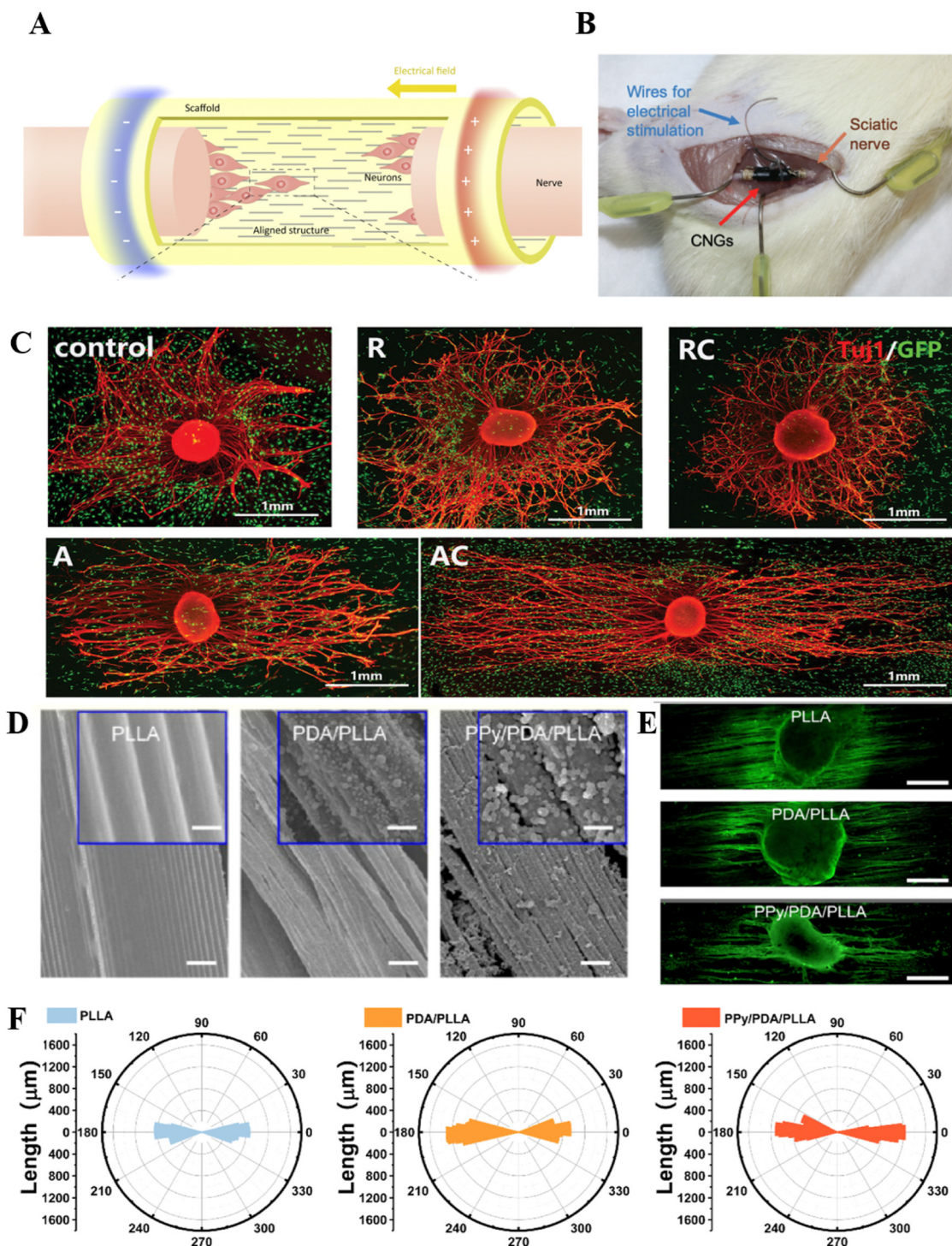


**Fig. 11** (A) Schematic diagram of the nerve conduit.<sup>12</sup> Copyright 2020 Elsevier Ltd. (B) Digital image of a nerve conduit implanted in a rat sciatic nerve transection model.<sup>160</sup> Copyright 2021 Elsevier Ltd. (C) Representative fluorescence staining images of DRGs protrusion growth co-cultured with induced BMSCs on nanofiber scaffolds, with Tuj1 labeled in red and GFP in green.<sup>163</sup> Copyright 2020 WILEY-VCH Verlag GmbH & Co. KGaA, Weinheim. (D) Surface topography of nanofibers with ordered arrangements: PLLA, PDA/PLLA, and PPY/PDA/PLLA nanofibers. Scale bars: 1  $\mu\text{m}$  (top) and 10  $\mu\text{m}$  (bottom). (E) Tuj1 immunofluorescence staining of dorsal root segments cultured *in vitro* on PPY/PDA/PLLA scaffolds with an ordered arrangement for 3 days. Scale bar: 500  $\mu\text{m}$ . (F) Polar histograms of neuronal protrusion direction, illustrating the alignment of neuromast growth from DRG cells along the fiber directions of PLLA, PDA/PLLA, and PPY/PDA/PLLA.<sup>159</sup> Copyright 2023 American Chemical Society.

stimulation, along with superior biocompatibility that promotes the proliferation and adhesion of neural cells, providing a new

design option for nerve conduits aimed at promoting peripheral nerve regeneration.



In the field of neural regeneration, nanostructured CPs must be implanted *in vivo* to directly contact tissues, necessitating non-toxicity and excellent biocompatibility. However, conventional synthesis methods often employ oxidizing agents (e.g.,  $\text{FeCl}_3$ ) or organic solvents (e.g., chloroform), which can introduce residual toxicity that is challenging to eliminate completely even after purification.<sup>44</sup> Additionally, ideal nerve conduits should gradually degrade after promoting nerve growth to prevent long-term foreign body reactions.<sup>167</sup> Conventional CPs, however, exhibit poor degradability and typically require compounding with other degradable materials.<sup>157</sup> During long-term degradation, maintaining the stability of the nanostructure is difficult, which may compromise its electrical conductivity. In the future, the *in vivo* degradability and conductivity of nanostructured CPs have to be balanced. On the other hand, highly ordered 3D porous structures or oriented nanofibers have been shown to effectively guide axon growth and cell migration.<sup>163,167</sup> The oriented CP nanofibers prepared by electrospinning can provide stable mechanical support and can effectively guide nerve axon growth.<sup>159</sup> In order to further meet the needs of nerve regeneration, the development of nanostructured CPs with controllable pore size, CP fiber arrangement or CPs with complex 3D morphology is necessary.

Nanostructured CPs play a unique role in neural regeneration, particularly in the form of oriented nanofibers and nerve conduits fabricated *via* electrospinning and 3D printing technologies. These materials can effectively mimic the structural and electrical signaling properties of natural neural tissues, thereby guiding axonal growth, promoting neuronal differentiation, and enhancing functional recovery. Despite these advances, several limitations persist. CPs are inherently poorly degradable and often require combination with degradable materials; however, maintaining nanostructure stability during long-term degradation is challenging, potentially weakening electrical conductivity and triggering foreign-body reactions. Traditional synthesis methods, which rely on oxidizing agents and organic solvents, introduce residual toxicity that poses safety hazards for *in vivo* implantation and cannot be fully eliminated by existing purification techniques. Additionally, CPs prepared by chemical oxidative polymerization face difficulties in precisely regulating porosity, fiber alignment, and complex 3D morphology, limiting their applicability in heterogeneous tissues. Future developments should focus on low-toxicity synthesis processes (e.g., green polymerization methods), smart degradation of CP composites, and incorporation of dynamic structural designs (e.g., stimuli-responsive materials) to balance electrical conductivity with biodegradability and biocompatibility.

### 3.4 Biosensors

A biosensor is a device that detects and converts physiological activities or biomolecules within an organism. It can monitor various biomarkers, hormones, proteins, and more, transforming the information into electrical or optical signals. This inherent capability significantly aids doctors and researchers in tracking disease progression and advancing scientific investigations.

Biosensors have a broad range of applications in medical diagnostics, biomedical research, and environmental monitoring.<sup>39,123,168</sup>

Biosensors usually consist of two interconnected components: a bioreceptor and a transducer. Early biosensors relied on the diffusion of the reaction product's concentration to generate an electrical response upon reaching the transducer, resulting in low sensitivity. Subsequently, sensors introduced a specific "medium" between the reactor and the transducer, employing a two-step process: first, a redox reaction occurs between the enzyme and substrate, followed by re-oxidation by a mediator, which is then oxidized by the electrode. In the latest generation of sensors, the redox reaction directly induces the response without relying on product diffusion or a medium. However, biomolecules exhibit a slow rate of electron transfer, limiting the electrochemical efficiency of these sensors. Therefore, there is an urgent need for efficient, user-friendly, and highly selective electrochemical biosensors.<sup>169</sup>

In contrast to conventional CPs, which are commonly used for electrochemical biosensor modification due to their unique conductivity, biosensors based on nanostructured CPs combine the benefits of intrinsic CPs with the advantages of nanostructuring. Firstly, the higher specific surface area and porous structure of nanostructured CPs increase the sensitivity and response of the sensor.<sup>170,171</sup> Secondly, the flexibility and biocompatibility of CPs enable biosensors to better adapt to the biological environment, minimizing damage to the organism.<sup>168</sup> Meanwhile, when combined with other materials, CPs can exhibit improved biocompatibility and biodegradability, reducing the risk of rejection and infection associated with implanted sensors. For example, Soni *et al.*<sup>170</sup> synthesized PANI nanotubes using a sacrificial template method and modified them onto an ITO substrate by electrophoretic deposition. They subsequently immobilized biotinylated DNA sequences between the CP nanotubes and the substrate using a cross-linking agent (Fig. 12(A)). In detecting chronic granulocytic leukemia, the biosensor exhibited a wide linear range, low detection limit, and enhanced discrimination and sensitivity, providing a new method for the clinical diagnosis of leukemia. Typically, electrochemical methods are employed to verify the sensitivity of the sensor regarding nuclear marker concentration, with differential pulse voltammetry (DPV) and cyclic voltammetry (CV) being commonly used techniques.<sup>164,172</sup> In one study, voltammetric modified electrodes featuring CP nanowires grown in porous materials were developed for the detection of carcinoembryonic antigen (CEA), a marker of colorectal adenocarcinoma. The DPV plot (Fig. 12(B)) reveals that the electrode modified with PANI/PEDOT/IL (curve b) showed a distinct DPV peak (peak potential of 0.16 V) compared to the unmodified electrode. Additionally, changes in CEA concentration affected the peak height. After immobilizing the non-conducting CEA antibody, the redox reaction of CPs was hindered, leading to a decrease in the DPV peak current. Thus, this potential can serve as a characteristic signal for CEA detection.<sup>172</sup> Nano-arrays leverage the advantages of one-dimensional nanowires or tubes with a highly ordered arrangement, enabling more effective utilization of nanostructured electrodes as enhancement elements. A miRNA biosensor was constructed using electrochemically synthesized polypyrrole





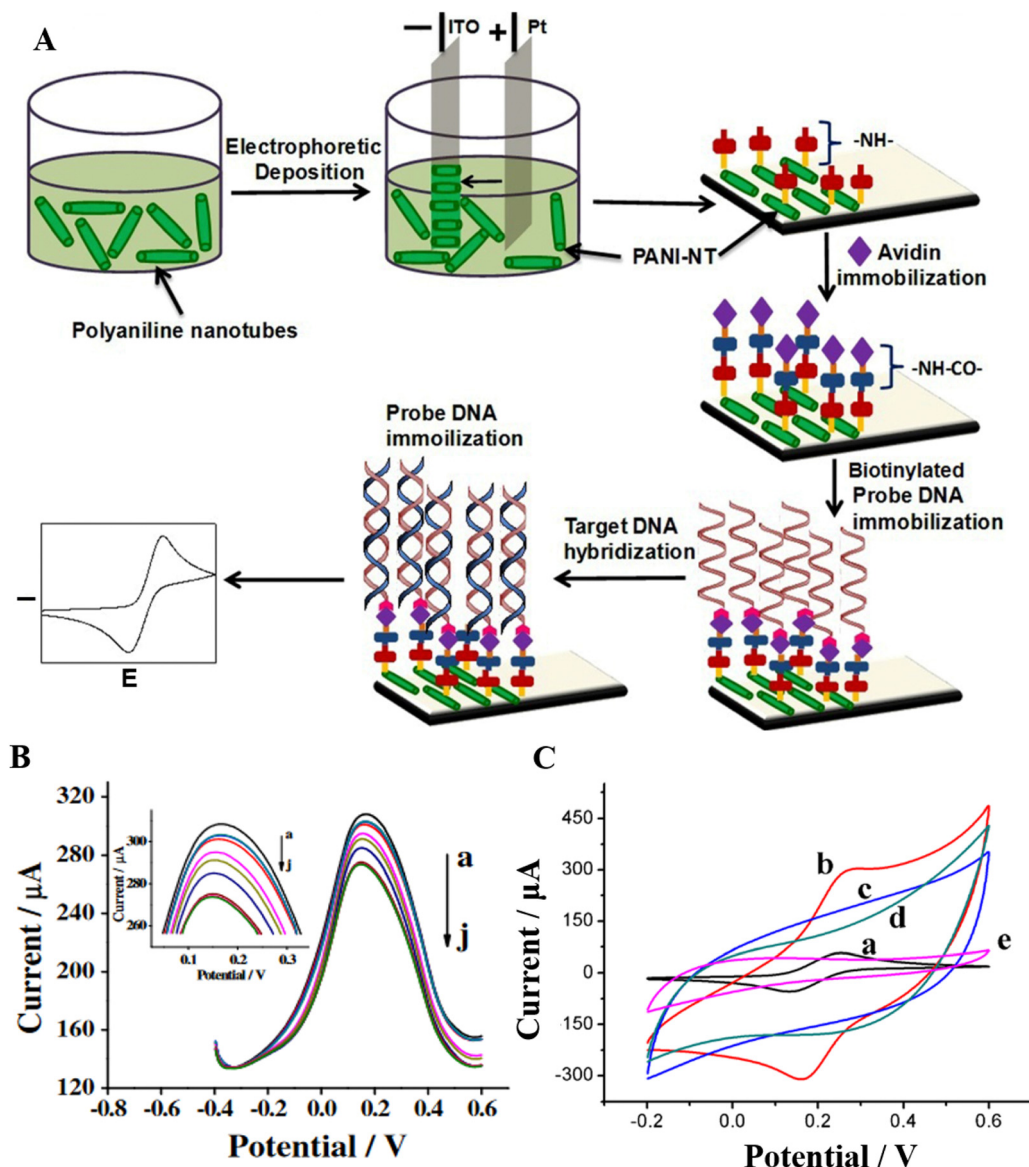


Fig. 12 (A) Schematic diagram of ordered PANI nanotubes electrophoretically deposited on an ITO electrode, resulting in the preparation of a pDNA/PANI-NT/ITO bioelectrode.<sup>170</sup> Copyright 2018 Elsevier B.V. (B) DPV response of the CP nanowire-modified electrode to different concentrations of CEA. Curve a represents a CEA concentration of  $0 \text{ g mL}^{-1}$ , while curves b–j correspond to concentrations ranging from  $10^{-14}$ – $10^{-6} \text{ GM L}^{-1}$ . Scanning potential:  $-0.4 \text{ V}$  to  $0.6 \text{ V}$ . Pulse amplitude:  $50 \text{ mV}$ , pulse width:  $50 \text{ ms}$ , sampling width:  $16.7 \text{ ms}$ .<sup>172</sup> Copyright 2017 Springer-Verlag Wien. (C) CV tests of different types of sensors in the presence of a mixed solution of  $0.1 \text{ M KCl}$  and  $5 \text{ mM } [\text{Fe}(\text{CN})_6]^{3/4-}$ . Curves a–e represent bare GCE, GCE/PPyNWs, GCE/PPyNWs/PAMAM, GCE/PPyNWs/PAMAM/DNA, and GCE/PPyNWs/PAMAM/DNA/RNA.<sup>172</sup> Copyright 2021 Springer Nature.

nanowires (PPy NWs), showcasing excellent sensing performance, a wide detection range, and a low detection limit. As shown by the CV test in Fig. 12(C), the biosensor exhibited a response sensitivity approximately 3.12 times higher than that of the sensor modified with CP film alone. This underscores the significant potential of ordered nanowire arrays to enhance biosensor performance.<sup>173</sup>

Wearable and smart medical technologies represent significant emerging trends in the field of biosensors, complementing the ongoing drive towards lower detection limits and enhanced sensitivity.<sup>174,175</sup> Within this context, Keirouz *et al.*<sup>175</sup> recently described a 3D-printed microneedle array coated with a conductive

polymer, offering a minimally invasive interface for biosensing applications. This development is noteworthy for its exceptional conductivity and biocompatibility, achieved in the absence of a metallic substrate. Moreover, 3D printing technology facilitates the cost-effective and customizable fabrication of microneedle arrays, thereby fostering the potential for future commercialization. The robust mechanical strength and effective skin penetration demonstrated by these arrays provide valuable insights for the advancement of next-generation wearable biosensors capable of real-time monitoring.

In practical applications like neural loop studies, detecting multiple target signals simultaneously is crucial, but most

existing techniques are limited to single analytes. To address this, researchers are developing multimodal sensors. For example, Wang *et al.* enhanced electrode performance by electrodepositing a composite of reduced graphene oxide and PEDOT:PSS, increasing surface roughness, reducing impedance, and achieving high sensitivity and selectivity in dopamine detection as well as a high signal-to-noise ratio for electrophysiological signals.<sup>176</sup> Xu *et al.* also prepared conductive PEDOT:PSS fibers *via* wet spinning, enabling successful electrochemical detection of dopamine and *in vivo* signal acquisition.<sup>177</sup> However, these advances are often confined to bimodal systems relying on specific redox peaks, limiting broader applications. Additionally, reducing interferences in complex biological samples, especially false positives, remains a challenge. Ni *et al.* tackled this by developing an aptamer-based GRP sensor for dopamine detection in the living brain, using a phosphorothioate aptamer to achieve high selectivity, stability, and reduced false positives.<sup>178</sup> These efforts highlight the urgent need to refine the preparation methods of nanostructured conducting polymers to improve their conductivity and enhance the performance and interference resistance of multimodal biosensors.

Nanostructured CPs enhance the sensitivity of biosensors through large specific surface areas and great biocompatibility, and the development of new technologies advances the clinical potential of noninvasive real-time monitoring. However, limitations still exist. Despite significant progress in the laboratory, the morphology and size distribution of nanostructures are difficult to precisely control in large-scale applications, affecting the consistency of device performance. Conductive polymers are prone to structural degradation or performance decay in repeated mechanical deformation, high temperature or oxidizing environments, making it difficult to maintain the nanostructure of CP. Maintaining sensor performance under extreme conditions is also a critical issue. Future research may be able to further improve the performance of sensors by designing bio-components that are resistant to extreme environments or by developing novel protective packaging techniques, thus facilitating the application of multimodal sensors in a wider range of fields.

## 4. Conclusion and outlook

Nanostructured CPs, encompassing nanofibers, nanotubes, and nanowires, have witnessed remarkable progress in synthetic methodologies, morphological control, physicochemical property modulation, and biomedical applications. This mini-review has delineated a spectrum of preparation techniques for nanostructured CPs, including but not limited to electrospinning, hard and soft templating, oriented electrochemical nanowire assembly, and dielectric electrophoresis, while also critically evaluating their respective merits and limitations. Despite these advancements, several fundamental challenges and promising future directions warrant in-depth consideration, particularly concerning their biomedical translation.

Electrical conductivity, while intrinsic to CPs, often faces compromises when integrated into biomedical systems.

The incorporation of non-conductive additives, frequently necessary for biocompatibility or functionalization, inevitably leads to a reduction in the overall conductivity of CP composites compared to their pristine counterparts. The root cause lies in the disruption of the continuous conductive pathways within the CP matrix by these insulating components. To address this, future research should prioritize strategies such as: (1) optimizing composite formulations: precisely controlling the ratio and dispersion of conductive and non-conductive phases to maintain sufficient conductivity while achieving desired bio-functionality. (2) Employing conductive additives: exploring conductive nanomaterials (*e.g.*, carbon nanotubes, graphene) as additives to compensate for conductivity loss and potentially enhance synergistic effects. (3) Interface engineering: modifying the interface between CPs and additives to improve charge transfer and minimize interfacial resistance.

Furthermore, a deeper understanding of fundamental charge transport mechanisms in nanostructured CPs, particularly at the nanoscale and in complex biological environments, is crucial. The intricate interplay between the nanostructure, electrical conductivity, and mechanical properties remains incompletely understood, hindering rational material design. Future investigations should emphasize: (1) advanced characterization techniques: employing advanced techniques such as nanoscale electrical characterization (*e.g.*, conductive AFM, scanning tunneling microscopy) and *in situ* characterization under physiological conditions to probe charge transport dynamics. (2) Theoretical modeling and simulation: developing and validating theoretical models to predict and explain charge transport behavior in nanostructured CPs, considering factors such as morphology, doping level, and environmental influences. (3) Structure-property relationship studies: systematically investigating the correlation between nanostructure parameters (*e.g.*, size, shape, and aspect ratio), electrical conductivity, mechanical properties, and bio-interfacial behavior to establish design principles for optimized performance.

Looking forward, nanostructured CPs are poised to revolutionize personalized medicine and intelligent medical devices, offering unprecedented opportunities in diagnostics, therapeutics, and monitoring. In diagnostics, CP-based nanosensors have great potential for real-time, highly sensitive, and minimally invasive biomarker detection. For instance, integrating nanostructured CPs into electrochemical or optical sensors could enable the rapid and accurate quantification of disease biomarkers (*e.g.*, glucose, proteins, and nucleic acids) in bodily fluids or tissues, facilitating early disease diagnosis and personalized treatment strategies. In therapeutics, nanostructured CPs can serve as versatile platforms for targeted drug delivery, gene therapy, and bioelectronic interfaces. Their unique electrical and photothermal properties can be exploited for controlled drug release triggered by electrical or light stimuli, enhancing therapeutic efficacy and minimizing off-target effects. Furthermore, CP-based bioelectronic interfaces can facilitate neural stimulation and recording, offering potential solutions for neurological disorders and neuroprosthetics.



In monitoring, the integration of nanostructured CPs into wearable and implantable devices can enable continuous and real-time health monitoring. CP-based wearable sensors can track physiological parameters (*e.g.*, heart rate, respiration, body temperature, and glucose levels) for proactive health management and disease prevention. Implantable CP devices can provide long-term monitoring of vital signs, drug levels, or disease progression, enabling personalized and adaptive healthcare interventions.

In conclusion, nanostructured CPs have transformative potential for biomedicine. By systematically addressing the aforementioned limitations and vigorously pursuing the proposed future research directions, we anticipate that nanostructured CPs will not only revolutionize healthcare through advanced diagnostics, therapeutics, and monitoring technologies but also significantly advance our fundamental understanding of bio-nano interactions and materials science. The journey from bench to bedside requires sustained interdisciplinary efforts, encompassing materials science, engineering, biology, and medicine, to fully realize the vast potential of nanostructured CPs for the benefit of human health.

## Abbreviations

AAO	Anodic aluminum oxide
ATP	Adenosine triphosphate
BMSCs	Bone marrow mesenchymal stem cells
CP	Conductive polymer
CNT	Carbon nanotube
CV	Cyclic voltammetry
CSA	Camphorsulfonic acid
CCD	Charge transfer capability and charge density
CEA	Carcinoembryonic antigen
C16TMA	Cetyltrimethylammonium chloride
DNA	Deoxyribonucleic acid
DOX	Doxorubicin
DPV	Differential pulse voltammetry
EDOT	Ethylene dioxythiophene
EISA	Evaporation-induced self-assembly
FE-SEM	Field emission scanning electron microscope
GOD	Glucose oxidase
HQS	8-Hydroxyquinoline-5-sulfonic acid
HCSA	(+)-Camphor-10-sulfonic acid
ITO	Indium tin oxide
MWCNTs	Multi-walled carbon nanotubes
MOFs	Metal-organic frameworks
MTX	Methotrexate
PA	Polyacetylene
PAN	Polyacrylonitrile
PANI	Polyaniline
PPY	Polypyrrole
PPY NWs	Polypyrrole nanowires
PT	Polythiophene
PEDOT	Poly(3,4-ethylenedioxythiophene)
P3HT	Poly(3-hexylthiophene)
P3TE	Poly(3-thiophenethanol)

PEO	Polyethylene oxide
PVDF	Polyvinylidene fluoride
PU	Polyurethane
PVP	Polyvinylpyrrolidone
PMMA	Polymethyl methacrylate
PHTNF	Poly(3-hexylthiophene) electrospinning nanofibers
PLGA	Poly(lactide-co-glycolide)
PLA	Poly(lactic acid)
PLLA	Poly-L-lactide
PCL	Poly-( $\epsilon$ -caprolactone)
PTMs	Particle size-etched membranes
PSS	Poly(4-sodium styrenesulfonate)
PC12-L	Pheochromocytoma
PDA	Polydopamine
SF	Silk fibroin
SDS	Sodium dodecyl sulfate
SCs	Schwann cells
TMV	Tobacco mosaic virus

## Data availability

No primary research results, software or code have been included and no new data were generated or analysed as part of this review.

## Conflicts of interest

The authors declare no competing financial interests.

## Acknowledgements

This work was financially supported by the Chinese Academy of Sciences (grant no. XDB0520301), the Basic Research Program of Jiangsu (grant no. BK20243004), and the Joint Open Research Fund of Suzhou Institute of Nano-Tech and Nano-Bionics & Jiangsu Province Hospital.

## References

- X.-X. Wang, G.-F. Yu, J. Zhang, M. Yu, S. Ramakrishna and Y.-Z. Long, Conductive polymer ultrafine fibers *via* electrospinning: Preparation, physical properties and applications, *Prog. Mater. Sci.*, 2021, **115**, 100704, DOI: [10.1016/j.pmatsci.2020.100704](https://doi.org/10.1016/j.pmatsci.2020.100704).
- Y. Yan, M. Han, Y. Jiang, E. L. L. Ng, Y. Zhang, C. Owh, Q. Song, P. Li, X. J. Loh, B. Q. Y. Chan and S. Y. Chan, Electrically conductive polymers for additive manufacturing, *ACS Appl. Mater. Interfaces*, 2024, **16**(5), 5337–5354, DOI: [10.1021/acsami.3c13258](https://doi.org/10.1021/acsami.3c13258).
- S. Bhattacharya, I. Roy, A. Tice, C. Chapman, R. Udangawa, V. Chakrapani, J. L. Plawsky and R. J. Linhardt, High-Conductivity and high-capacitance electrospun fibers for supercapacitor applications, *ACS Appl. Mater. Interfaces*, 2020, **12**(17), 19369–19376, DOI: [10.1021/acsami.9b21696](https://doi.org/10.1021/acsami.9b21696).



- 4 M. Acosta, M. D. Santiago and J. A. Irvin, Electrospun conducting polymers: Approaches and applications, *Materials*, 2022, **15**, 8820, DOI: [10.3390/ma15248820](#).
- 5 Y.-Z. Long, M.-M. Li, C. Gu, M. Wan, J.-L. Duvail, Z. Liu and Z. Fan, Recent advances in synthesis, physical properties and applications of conducting polymer nanotubes and nanofibers, *Prog. Polym. Sci.*, 2011, **36**(10), 1415–1442, DOI: [10.1016/j.progpolymsci.2011.04.001](#).
- 6 S.-Y. Jang, V. Seshadri, M.-S. Khil, A. Kumar, M. Marquez, P. T. Mather and G. A. Sotzing, Welded electrochromic conductive polymer nanofibers by electrostatic spinning, *Adv. Mater.*, 2005, **17**(18), 2177–2180, DOI: [10.1002/adma.200500577](#).
- 7 N. Zarrin, H. Tavanai, A. Abdolmaleki, M. Bazarganipour and F. Alihosseini, An investigation on the fabrication of conductive polyethylene dioxythiophene (PEDOT) nanofibers through electrospinning, *Synth. Met.*, 2018, **244**, 143–149, DOI: [10.1016/j.synthmet.2018.07.013](#).
- 8 Y. Ziai, S. S. Zargarian, C. Rinoldi, P. Nakielski, A. Sola, M. Lanzi, Y. B. Truong and F. Pierini, Conducting polymer-based nanostructured materials for brain-machine interfaces, *Wiley Interdiscip. Rev.: Nanomed. Nanobiotechnol.*, 2023, **15**(5), e1895, DOI: [10.1002/wnan.1895](#).
- 9 V. Datsyuk, S. Trotsenko and S. Reich, Carbon-Nanotube-Polymer nanofibers with high thermal conductivity, *Carbon*, 2013, **52**, 605–608, DOI: [10.1016/j.carbon.2012.09.045](#).
- 10 L. Wei, S. Wang, M. Shan, Y. Li, Y. Wang, F. Wang, L. Wang and J. Mao, Conductive fibers for biomedical applications, *Bioact. Mater.*, 2023, **22**, 343–364, DOI: [10.1016/j.bioactmat.2022.10.014](#).
- 11 P. Moutsatsou, K. Coopman, M. B. Smith and S. Georgiadou, Conductive PANI fibers and determining factors for the electrospinning window, *Polymer*, 2015, **77**, 143–151, DOI: [10.1016/j.polymer.2015.08.039](#).
- 12 Y. Zhao, Y. Liang, S. Ding, K. Zhang, H. Mao and Y. Yang, Application of conductive PPY/SF composite scaffold and electrical stimulation for neural tissue engineering, *Biomaterials*, 2020, **255**, 120164, DOI: [10.1016/j.biomaterials.2020.120164](#).
- 13 X. Lu, W. Zhang, C. Wang, T.-C. Wen and Y. Wei, One-Dimensional conducting polymer nanocomposites: Synthesis, properties and applications, *Prog. Polym. Sci.*, 2011, **36**(5), 671–712, DOI: [10.1016/j.progpolymsci.2010.07.010](#).
- 14 H. Xu, J. M. Holzwarth, Y. Yan, P. Xu, H. Zheng, Y. Yin, S. Li and P. X. Ma, Conductive PPY/PDLLA conduit for peripheral nerve regeneration, *Biomaterials*, 2014, **35**(1), 225–235, DOI: [10.1016/j.biomaterials.2013.10.002](#).
- 15 R. González and N. J. Pinto, Electrospun poly(3-Hexylthiophene-2,5-Diyl) fiber field effect transistor, *Synth. Met.*, 2005, **151**(3), 275–278, DOI: [10.1016/j.synthmet.2005.05.007](#).
- 16 Y. Zhang, J. J. Kim, D. Chen, H. L. Tuller and G. C. Rutledge, Electrospun polyaniline fibers as highly sensitive room temperature chemiresistive sensors for ammonia and nitrogen dioxide gases, *Adv. Funct. Mater.*, 2014, **24**(25), 4005–4014, DOI: [10.1002/adfm.201400185](#).
- 17 Q.-Z. Yu, M.-M. Shi, M. Deng, M. Wang and H.-Z. Chen, Morphology and conductivity of polyaniline sub-micron fibers prepared by electrospinning, *Mater. Sci. Eng., B*, 2008, **150**(1), 70–76, DOI: [10.1016/j.mseb.2008.02.008](#).
- 18 H. Liu, C. H. Reccius and H. G. Craighead, Single Electrospun regioregular poly(3-hexylthiophene) nanofiber field-effect transistor, *Appl. Phys. Lett.*, 2005, **87**(25), 253106, DOI: [10.1063/1.2149980](#).
- 19 X. Hou, Y. Zhou, Y. Liu, L. Wang and J. Wang, Coaxial electrospun flexible PANI//PU fibers as highly sensitive pH wearable sensor, *J. Mater. Sci.*, 2020, **55**(33), 16033–16047, DOI: [10.1007/s10853-020-05110-7](#).
- 20 A. Sarvi, V. Chimello, A. B. Silva, R. E. S. Bretas and U. Sundararaj, Coaxial electrospun nanofibers of poly(vinylidene fluoride)/polyaniline filled with multi-walled carbon nanotubes, *Polym. Compos.*, 2014, **35**(6), 1198–1203, DOI: [10.1002/pc.22768](#).
- 21 Y. Srivastava, I. Loscertales, M. Marquez and T. Thorsen, Electrospinning of hollow and core/sheath nanofibers using a microfluidic manifold, *Microfluid. Nanofluid.*, 2008, **4**(3), 245–250, DOI: [10.1007/s10404-007-0177-0](#).
- 22 J. Chen, H. Wu, Y. Chiu, C. Lin, S. Tung and W. Chen, Electrospun poly(3-hexylthiophene) nanofibers with highly extended and oriented chains through secondary electric field for high-performance field-effect transistors, *Adv. Electron. Mater.*, 2015, **1**(1–2), 1400028, DOI: [10.1002/aelm.201400028](#).
- 23 J.-Y. Chen, C.-C. Kuo, C.-S. Lai, W.-C. Chen and H.-L. Chen, Manipulation on the morphology and electrical properties of aligned electrospun nanofibers of poly(3-hexylthiophene) for field-effect transistor applications, *Macromolecules*, 2011, **44**(8), 2883–2892, DOI: [10.1021/ma102286m](#).
- 24 D. Li, A. Babel, S. A. Jenekhe and Y. Xia, Nanofibers of conjugated polymers prepared by electrospinning with a two-capillary spinneret, *Adv. Mater.*, 2004, **16**(22), 2062–2066, DOI: [10.1002/adma.200400606](#).
- 25 N. M. Bedford and A. J. Steckl, Photocatalytic self cleaning textile fibers by coaxial electrospinning, *ACS Appl. Mater. Interfaces*, 2010, **2**(8), 2448–2455, DOI: [10.1021/am1005089](#).
- 26 C.-J. Lin, C.-L. Liu and W.-C. Chen, Poly(3-Hexylthiophene)-Graphene composite-based aligned nanofibers for high-performance field effect transistors, *J. Mater. Chem. C*, 2015, **3**(17), 4290–4296, DOI: [10.1039/C5TC00399G](#).
- 27 M. Lin, T. Don, F. Chang, S. Huang and W. Chiu, Preparation and properties of thermoresponsive and conductive composite fibers with core-sheath structure, *J. Polym. Sci. Part A: Polym. Chem.*, 2016, **54**(9), 1299–1307, DOI: [10.1002/pola.27976](#).
- 28 Y. Liang, A. Mitriashkin, T. T. Lim and J. C.-H. Goh, Conductive polypyrrole-encapsulated silk fibroin fibers for cardiac tissue engineering, *Biomaterials*, 2021, **276**, 121008, DOI: [10.1016/j.biomaterials.2021.121008](#).
- 29 M. E. Spiers, D. J. Nielsen, K. D. Pavey, Y. B. Truong, G. C. Rutledge, P. Kingshott and D. S. Eldridge, Conductive, Acid-Doped polyaniline electrospun nanofiber gas sensing substrates made using a facile dissolution method, *ACS Appl. Mater. Interfaces*, 2021, **13**(44), 52950–52959, DOI: [10.1021/acsami.1c08136](#).





- 30 M. P. Prabhakaran, L. Ghasemi-Mobarakeh and S. Ramakrishna, Electrospun composite nanofibers for tissue regeneration, *J. Nanosci. Nanotech.*, 2011, **11**(4), 3039–3057, DOI: [10.1166/jnn.2011.3753](#).
- 31 Q. Xu, Y. Li, W. Feng and X. Yuan, Fabrication and electrochemical properties of polyvinyl alcohol/poly(3,4-ethylenedioxythiophene) ultrafine fibers *via* electrospinning of EDOT monomers with subsequent *in situ* polymerization, *Synth. Met.*, 2010, **160**(1–2), 88–93, DOI: [10.1016/j.synthmet.2009.10.010](#).
- 32 B. Bessaire, M. Mathieu, V. Salles, T. Yeghoyan, C. Celle, J.-P. Simonato and A. Brioude, Synthesis of continuous conductive PEDOT:PSS nanofibers by electrospinning: A conformal coating for optoelectronics, *ACS Appl. Mater. Interfaces*, 2017, **9**(1), 950–957, DOI: [10.1021/acsami.6b13453](#).
- 33 B. K. Gu, Y. A. Ismail, G. M. Spinks, S. I. Kim, I. So and S. J. Kim, A linear actuation of polymeric nanofibrous bundle for artificial muscles, *Chem. Mater.*, 2009, **21**(3), 511–515, DOI: [10.1021/cm802377d](#).
- 34 S. Demirci Uzun, F. Kayaci, T. Uyar, S. Timur and L. Toppare, Bioactive surface design based on functional composite electrospun nanofibers for biomolecule immobilization and biosensor applications, *ACS Appl. Mater. Interfaces*, 2014, **6**(7), 5235–5243, DOI: [10.1021/am5005927](#).
- 35 M. R. Abidian, D.-H. Kim and D. C. Martin, Conducting-Polymer nanotubes for controlled drug release, *Adv. Mater.*, 2006, **18**(4), 405–409, DOI: [10.1002/adma.200501726](#).
- 36 M. R. Abidian, J. M. Corey, D. R. Kipke and D. C. Martin, Conducting-Polymer nanotubes improve electrical properties, mechanical adhesion, neural attachment, and neurite outgrowth of neural electrodes, *Small*, 2010, **6**(3), 421–429, DOI: [10.1002/smll.200901868](#).
- 37 F. Zha, W. Chen, G. Lv, C. Wu, L. Hao, L. Meng, L. Zhang and D. Yu, Effects of surface condition of conductive electrospun nanofiber mats on cell behavior for nerve tissue engineering, *Mater. Sci. Eng., C*, 2021, **120**, 111795, DOI: [10.1016/j.msec.2020.111795](#).
- 38 A. Attout, S. Yunus and P. Bertrand, Electrospinning and alignment of polyaniline-based nanowires and nanotubes, *Polym. Eng. Sci.*, 2008, **48**(9), 1661–1666, DOI: [10.1002/pen.20969](#).
- 39 M. R. Abidian and D. C. Martin, Experimental and theoretical characterization of implantable neural microelectrodes modified with conducting polymer nanotubes, *Biomaterials*, 2008, **29**(9), 1273–1283, DOI: [10.1016/j.biomaterials.2007.11.022](#).
- 40 F. Miao, C. Shao, X. Li, K. Wang and Y. Liu, Flexible solid-state supercapacitors based on freestanding nitrogen-doped porous carbon nanofibers derived from electrospun polyacrylonitrile@polyaniline nanofibers, *J. Mater. Chem. A*, 2016, **4**(11), 4180–4187, DOI: [10.1039/C6TA00015K](#).
- 41 Y.-E. Miao, W. Fan, D. Chen and T. Liu, High-Performance supercapacitors based on hollow polyaniline nanofibers by electrospinning, *ACS Appl. Mater. Interfaces*, 2013, **5**(10), 4423–4428, DOI: [10.1021/am4008352](#).
- 42 Z.-Q. Feng, J. Wu, W. Cho, M. K. Leach, E. W. Franz, Y. I. Naim, Z.-Z. Gu, J. M. Corey and D. C. Martin, Highly aligned poly(3,4-ethylene dioxythiophene) (PEDOT) nano- and microscale fibers and tubes, *Polymer*, 2013, **54**(2), 702–708, DOI: [10.1016/j.polymer.2012.10.057](#).
- 43 S. Pantalei, E. Zampetti, A. Bearzotti, F. De Cesare and A. Macagnano, Improving sensing features of a nanocomposite PEDOT:PSS sensor for NO breath monitoring, *Sens. Actuators B: Chem.*, 2013, **179**, 87–94, DOI: [10.1016/j.snb.2012.10.015](#).
- 44 M. R. Abidian, K. A. Ludwig, T. C. Marzullo, D. C. Martin and D. R. Kipke, Interfacing conducting polymer nanotubes with the central nervous system: Chronic neural recording using poly(3,4-ethylenedioxythiophene) nanotubes, *Adv. Mater.*, 2009, **21**(37), 3764–3770, DOI: [10.1002/adma.200900887](#).
- 45 M. R. Abidian and D. C. Martin, Multifunctional nanobio-materials for neural interfaces, *Adv. Funct. Mater.*, 2009, **19**(4), 573–585, DOI: [10.1002/adfm.200801473](#).
- 46 N. Chen, B. Luo, A. C. Patil, J. Wang, G. G. L. Gammad, Z. Yi, X. Liu, S.-C. Yen, S. Ramakrishna and N. V. Thakor, Nanotunnels within poly(3,4-ethylenedioxythiophene)-carbon nanotube composite for highly sensitive neural interfacing, *ACS Nano*, 2020, **14**(7), 8059–8073, DOI: [10.1021/acsnano.0c00672](#).
- 47 J. Y. Lee, C. A. Bashur, A. S. Goldstein and C. E. Schmidt, Polypyrrole-Coated electrospun PLGA nanofibers for neural tissue applications, *Biomaterials*, 2009, **30**(26), 4325–4335, DOI: [10.1016/j.biomaterials.2009.04.042](#).
- 48 A. Macagnano, A. Bearzotti, F. De Cesare and E. Zampetti, Sensing asthma with portable devices equipped with ultrasensitive sensors based on electrospun nanomaterials, *Electroanalysis*, 2014, **26**(6), 1419–1429, DOI: [10.1002/elan.201400067](#).
- 49 H. Dong, S. Prasad, V. Nyame and W. E. Jones, Sub-Micrometer conducting polyaniline tubes prepared from polymer fiber templates, *Chem. Mater.*, 2004, **16**(3), 371–373, DOI: [10.1021/cm0347180](#).
- 50 Y. Li, J. Gong, G. He and Y. Deng, Synthesis of polyaniline nanotubes using Mn<sub>2</sub>O<sub>3</sub> nanofibers as oxidant and their ammonia sensing properties, *Synth. Met.*, 2011, **161**(1–2), 56–61, DOI: [10.1016/j.synthmet.2010.10.034](#).
- 51 E. Zampetti, S. Pantalei, A. Bearzotti, C. Bongiorno, F. De Cesare, C. Spinella and A. Macagnano, TiO<sub>2</sub> nanofibrous chemoresistors coated with PEDOT and PANi blends for high performance gas sensors, *Procedia Eng.*, 2012, **47**, 937–940, DOI: [10.1016/j.proeng.2012.09.300](#).
- 52 W. Wang, Z. Li, X. Xu, B. Dong, H. Zhang, Z. Wang, C. Wang, R. H. Baughman and S. Fang, Au-Doped polyacrylonitrile–polyaniline core–shell electrospun nanofibers having high field-effect mobilities, *Small*, 2011, **7**(5), 597–600, DOI: [10.1002/smll.201001716](#).
- 53 F. Zhang, Y. Xia, L. Wang, L. Liu, Y. Liu and J. Leng, Conductive shape memory microfiber membranes with core–shell structures and electroactive performance, *ACS Appl. Mater. Interfaces*, 2018, **10**(41), 35526–35532, DOI: [10.1021/acsami.8b12743](#).



- 54 J. Liu, D. L. McCarthy, L. Tong, M. J. Cowan, J. M. Kinsley, L. Sonnenberg, K. H. Skorenko, S. M. Boyer, J. B. DeCoste, W. E. Bernier and W. E. Jones, Poly(3,4-Ethylenedioxythiophene) (PEDOT) infused TiO<sub>2</sub> nanofibers: The role of hole transport layer in photocatalytic degradation of phenazopyridine as a pharmaceutical contaminant, *RSC Adv.*, 2016, **6**(115), 113884, DOI: [10.1039/C6RA22797J](https://doi.org/10.1039/C6RA22797J).
- 55 S. Li, X. Lu, X. Li, Y. Xue, C. Zhang, J. Lei and C. Wang, Preparation of bamboo-like PPy nanotubes and their application for removal of Cr(VI) ions in aqueous solution, *J. Colloid Interface Sci.*, 2012, **378**(1), 30–35, DOI: [10.1016/j.jcis.2012.03.065](https://doi.org/10.1016/j.jcis.2012.03.065).
- 56 A. Laforgue and L. Robitaille, Production of conductive PEDOT nanofibers by the combination of electrospinning and vapor-phase polymerization, *Macromolecules*, 2010, **43**(9), 4194–4200, DOI: [10.1021/ma9027678](https://doi.org/10.1021/ma9027678).
- 57 P. Chen, X. Shang and T. Hang, Capillary-Assisted assembly of soft conductive polymer nanopillar/tube arrays and applications, *Nano Lett.*, 2024, **24**(4), 1423–1430, DOI: [10.1021/acs.nanolett.3c04880](https://doi.org/10.1021/acs.nanolett.3c04880).
- 58 Z. Niu, J. Liu, L. A. Lee, M. A. Bruckman, D. Zhao, G. Koley and Q. Wang, Biological templated synthesis of water-soluble conductive polymeric nanowires, *Nano Lett.*, 2007, **7**(12), 3729–3733, DOI: [10.1021/nl072134h](https://doi.org/10.1021/nl072134h).
- 59 D. Gan, L. Han, M. Wang, W. Xing, T. Xu, H. Zhang, K. Wang, L. Fang and X. Lu, Conductive and tough hydrogels based on biopolymer molecular templates for controlling *in situ* formation of polypyrrole nanorods, *ACS Appl. Mater. Interfaces*, 2018, **10**(42), 36218–36228, DOI: [10.1021/acsami.8b10280](https://doi.org/10.1021/acsami.8b10280).
- 60 J. Xie, M. R. MacEwan, S. M. Willerth, X. Li, D. W. Moran, S. E. Sakiyama-Elbert and Y. Xia, Conductive core–sheath nanofibers and their potential application in neural tissue engineering, *Adv. Funct. Mater.*, 2009, **19**(14), 2312–2318, DOI: [10.1002/adfm.200801904](https://doi.org/10.1002/adfm.200801904).
- 61 F. Hu, B. Yan, G. Sun, J. Xu, Y. Gu, S. Lin, S. Zhang, B. Liu and S. Chen, Conductive polymer nanotubes for electrochromic applications, *ACS Appl. Nano Mater.*, 2019, **2**(5), 3154–3160, DOI: [10.1021/acsanm.9b00472](https://doi.org/10.1021/acsanm.9b00472).
- 62 S. M. D. Watson, A. R. Pike, J. Pate, A. Houlton and B. R. Horrocks, DNA-Templated nanowires: Morphology and electrical conductivity, *Nanoscale*, 2014, **6**(8), 4027–4037, DOI: [10.1039/C3NR06767J](https://doi.org/10.1039/C3NR06767J).
- 63 F. Massuyeau, J. Duvail, H. Athalin, J. Lorcy, S. Lefrant, J. Wéry and E. Faulques, Elaboration of conjugated polymer nanowires and nanotubes for tunable photoluminescence properties, *Nanotechnology*, 2009, **20**(15), 155701, DOI: [10.1088/0957-4484/20/15/155701](https://doi.org/10.1088/0957-4484/20/15/155701).
- 64 H. Xie, S. Luo and H. Yu, Electric-Field-Assisted growth of functionalized poly(3,4-ethylenedioxythiophene) nanowires for label-free protein detection, *Small*, 2009, **5**(22), 2611–2617, DOI: [10.1002/smll.200900312](https://doi.org/10.1002/smll.200900312).
- 65 Y. Long, J. Duvail, Z. Chen, A. Jin and C. Gu, Electrical properties of isolated poly(3,4-ethylenedioxythiophene) nanowires prepared by template synthesis, *Polym. Adv. Technol.*, 2009, **20**(6), 541–544, DOI: [10.1002/pat.1379](https://doi.org/10.1002/pat.1379).
- 66 V. Callegari, L. Gence, S. Melinte and S. Demoustier-Champagne, Electrochemically template-grown multi-segmented gold-conducting polymer nanowires with tunable electronic behavior, *Chem. Mater.*, 2009, **21**(18), 4241–4247, DOI: [10.1021/cm901224u](https://doi.org/10.1021/cm901224u).
- 67 D. K. Taggart, Y. Yang, S.-C. Kung, T. M. McIntire and R. M. Penner, Enhanced thermoelectric metrics in ultra-long electrodeposited PEDOT nanowires, *Nano Lett.*, 2011, **11**(1), 125–131, DOI: [10.1021/nl103003d](https://doi.org/10.1021/nl103003d).
- 68 M.-S. She and R.-M. Ho, Formation of conductive polyaniline nanoarrays from block copolymer template *via* electroplating, *Polymer*, 2012, **53**(13), 2628–2632, DOI: [10.1016/j.polymer.2012.04.031](https://doi.org/10.1016/j.polymer.2012.04.031).
- 69 T. Wang, M. Farajollahi, S. Henke, T. Zhu, S. R. Bajpe, S. Sun, J. S. Barnard, J. S. Lee, J. D. W. Madden, A. K. Cheetham and S. K. Smoukov, Functional conductive nanomaterials *via* polymerisation in nano-channels: PEDOT in a MOF, *Mater. Horiz.*, 2017, **4**(1), 64–71, DOI: [10.1039/C6MH00230G](https://doi.org/10.1039/C6MH00230G).
- 70 Y. Dan, Y. Cao, T. Mallouk, S. Evoy and A. Johnson, Gas sensing properties of single conducting polymer nanowires and the effect of temperature, *Nanotechnology*, 2009, **20**(43), 434014, DOI: [10.1088/0957-4484/20/43/434014](https://doi.org/10.1088/0957-4484/20/43/434014).
- 71 M. Bhuyan, F. Courvoisier, P. Lacourt, M. Jacquot, R. Salut, L. Furfaro and J. Dudley, High aspect ratio nanochannel machining using single shot femtosecond bessel beams, *Appl. Phys. Lett.*, 2010, **97**(8), 081102, DOI: [10.1063/1.3479419](https://doi.org/10.1063/1.3479419).
- 72 V. Callegari and S. Demoustier-Champagne, Interfacing conjugated polymers with magnetic nanowires, *ACS Appl. Mater. Interfaces*, 2010, **2**(5), 1369–1376, DOI: [10.1021/am100023k](https://doi.org/10.1021/am100023k).
- 73 R. Liu and S. B. Lee, MnO<sub>2</sub>/Poly(3,4-Ethylenedioxythiophene) coaxial nanowires by one-step coelectrodeposition for electrochemical energy storage, *J. Am. Chem. Soc.*, 2008, **130**(10), 2942–2943, DOI: [10.1021/ja7112382](https://doi.org/10.1021/ja7112382).
- 74 C. R. Martin, Nanomaterials: A membrane-based synthetic approach, *Science*, 1994, **266**(5193), 1961–1966, DOI: [10.1126/science.266.5193.1961](https://doi.org/10.1126/science.266.5193.1961).
- 75 J. Zhang, S. Zhu, Y. Sun, Y. Dang, Z. Song and L. Zhang, Doping P heteroatoms into thin-wall polypyrrole hollow nanobelts with enhanced electrochemical performance for aqueous Zn ion storage, *J. Electroanal. Chem.*, 2024, **967**, 118483, DOI: [10.1016/j.jelechem.2024.118483](https://doi.org/10.1016/j.jelechem.2024.118483).
- 76 H. Tran, D. Li and R. Kaner, One-Dimensional conducting polymer nanostructures: Bulk synthesis and applications, *Adv. Mater.*, 2009, **21**(14–15), 1487–1499, DOI: [10.1002/adma.200802289](https://doi.org/10.1002/adma.200802289).
- 77 S. Trakhtenberg, Y. Hangan-Balkir, J. C. Warner, F. F. Bruno, J. Kumar, R. Nagarajan and L. A. Samuelson, Photo-Cross-Linked immobilization of polyelectrolytes for enzymatic construction of conductive nanocomposites, *J. Am. Chem. Soc.*, 2005, **127**(25), 9100–9104, DOI: [10.1021/ja042343v](https://doi.org/10.1021/ja042343v).
- 78 J. Kim, S. Kim and K. Yoo, Polypyrrole nanowire-based enzymatic biofuel cells, *Biosens. Bioelectron.*, 2009, **25**(2), 350–355, DOI: [10.1016/j.bios.2009.07.020](https://doi.org/10.1016/j.bios.2009.07.020).



- 79 Y. Chen and Y. Luo, Precisely defined heterogeneous conducting polymer nanowire arrays - fabrication and chemical sensing applications, *Adv. Mater.*, 2009, **21**(20), 2040–2044, DOI: [10.1002/adma.200803292](https://doi.org/10.1002/adma.200803292).
- 80 Y. Wan, N. Qin, Y. Wang, Q. Zhao, Q. Wang, P. Yuan, Q. Wen, H. Wei, X. Zhang and N. Ma, Sugar-Templated conductive polyurethane-polypyrrole sponges for wide-range force sensing, *Chem. Eng. J.*, 2020, **383**, 123103, DOI: [10.1016/j.cej.2019.123103](https://doi.org/10.1016/j.cej.2019.123103).
- 81 C.-H. Liu, S. Krueger and M.-P. Nieh, Synthesis of polymer nanoweb via a lipid template, *ACS Macro Lett.*, 2023, **12**(7), 993–998, DOI: [10.1021/acsmacrolett.3c00255](https://doi.org/10.1021/acsmacrolett.3c00255).
- 82 Z. Wu, Y. Wu, L. Yang, X. Zuo, Z. Wang, Y. Yan, W. Li, D. Chang, Y. Guo, X. Mo, X. Lu, Y. Liu and Y. Zhao, Template-Assisted fabrication of single-crystal-like polymer fibers for efficient charge transport, *Adv. Fiber Mater.*, 2023, **5**(6), 2069–2079, DOI: [10.1007/s42765-023-00326-z](https://doi.org/10.1007/s42765-023-00326-z).
- 83 X. Li, M. Wan, X. Li and G. Zhao, The role of DNA in PANI-DNA hybrid: Template and dopant, *Polymer*, 2009, **50**(19), 4529–4534, DOI: [10.1016/j.polymer.2009.07.024](https://doi.org/10.1016/j.polymer.2009.07.024).
- 84 J. Rong, F. Oberbeck, X. Wang, X. Li, J. Oxsher, Z. Niu and Q. Wang, Tobacco mosaic virus templated synthesis of one dimensional inorganic–polymer hybrid fibres, *J. Mater. Chem.*, 2009, **19**(18), 2841, DOI: [10.1039/b901130g](https://doi.org/10.1039/b901130g).
- 85 V. Callegari and S. Demoustier-Champagne, Using the hard templating method for the synthesis of metal-conducting polymer multi-segmented nanowires, *Macromol. Rapid Commun.*, 2011, **32**(1), 25–34, DOI: [10.1002/marc.201000486](https://doi.org/10.1002/marc.201000486).
- 86 T. Dai and Y. Lu, Water-Soluble methyl orange fibrils as versatile templates for the fabrication of conducting polymer microtubules, *Macromol. Rapid Commun.*, 2007, **28**(5), 629–633, DOI: [10.1002/marc.200600697](https://doi.org/10.1002/marc.200600697).
- 87 Y. Chen and Y. Li, Conductive and sensing performance of polypyrrole composited elastic filaments by template synthesis, *J. Text. Inst.*, 2022, **113**(6), 1114–1122, DOI: [10.1080/00405000.2021.1915587](https://doi.org/10.1080/00405000.2021.1915587).
- 88 S. Park, T.-G. Kwon, S.-I. Park, S. Kim, J. Kwak and S.-Y. Lee, Conductive microrod preparation by molecular self-assembly and polymerization, *RSC Adv.*, 2013, **3**(22), 8468, DOI: [10.1039/c3ra40250a](https://doi.org/10.1039/c3ra40250a).
- 89 Y. Wang, K. Cai and X. Yao, Facile fabrication and thermoelectric properties of PbTe-modified poly(3,4-ethylenedioxythiophene) nanotubes, *ACS Appl. Mater. Interfaces*, 2011, **3**(4), 1163–1166, DOI: [10.1021/am101287w](https://doi.org/10.1021/am101287w).
- 90 M. G. Han and S. H. Foulger, Facile synthesis of poly(3,4-ethylenedioxythiophene) nanofibers from an aqueous surfactant solution, *Small*, 2006, **2**(10), 1164–1169, DOI: [10.1002/sml.200600135](https://doi.org/10.1002/sml.200600135).
- 91 K. Su, N. Nuraje, L. Zhang, I.-W. Chu, R. M. Peetz, H. Matsui and N.-L. Yang, Fast conductance switching in single-crystal organic nanoneedles prepared from an interfacial polymerization-crystallization of 3,4-ethylenedioxythiophene, *Adv. Mater.*, 2007, **19**(5), 669–672, DOI: [10.1002/adma.200602277](https://doi.org/10.1002/adma.200602277).
- 92 H.-H. Liu, M.-Q. Zhang, Z.-H. Tian, P.-F. Liu, Y.-X. Liu and X.-X. Zhang, Flexible thermoelectric nanodevices based on three-dimensional networks of poly(3,4-ethylenedioxythiophene) nanowires and graphene, *High Perform. Polym.*, 2021, **33**(6), 657–664, DOI: [10.1177/0954008320974432](https://doi.org/10.1177/0954008320974432).
- 93 D. Ni, Y. Chen, H. Song, C. Liu, X. Yang and K. Cai, Free-Standing and highly conductive PEDOT nanowire films for high-performance all-solid-state supercapacitors, *J. Mater. Chem. A*, 2019, **7**(3), 1323–1333, DOI: [10.1039/C8TA08814D](https://doi.org/10.1039/C8TA08814D).
- 94 D. Ni, H. Song, Y. Chen and K. Cai, Free-Standing highly conducting PEDOT films for flexible thermoelectric generator, *Energy*, 2019, **170**, 53–61, DOI: [10.1016/j.energy.2018.12.124](https://doi.org/10.1016/j.energy.2018.12.124).
- 95 J. Huang and R. B. Kaner, Nanofiber formation in the chemical polymerization of aniline: A mechanistic study, *Angew. Chem., Int. Ed.*, 2004, **43**(43), 5817–5821, DOI: [10.1002/anie.200460616](https://doi.org/10.1002/anie.200460616).
- 96 A. Subramania and S. L. Devi, Polyaniline nanofibers by surfactant-assisted dilute polymerization for supercapacitor applications, *Polym. Adv. Technol.*, 2008, **19**(7), 725–727, DOI: [10.1002/pat.1016](https://doi.org/10.1002/pat.1016).
- 97 H. Guo, J. Chen and Y. Xu, Protein-Induced synthesis of chiral conducting polyaniline nanospheres, *ACS Macro Lett.*, 2014, **3**(4), 295–297, DOI: [10.1021/mz500008f](https://doi.org/10.1021/mz500008f).
- 98 T. Bahry, Z. Cui, A. Dazzi, M. Gervais, C. Sollogoub, F. Goubard, T.-T. Bui and S. Remita, Radiation-Induced polymerization of 3-hexylthiophene in oxygen-free and oxygen-saturated dichloromethane solvent, *Radiat. Phys. Chem.*, 2021, **180**, 109291, DOI: [10.1016/j.radphyschem.2020.109291](https://doi.org/10.1016/j.radphyschem.2020.109291).
- 99 L. Lv, Y. Zhao, N. Vilbrandt, M. Gallei, A. Vimalanandan, M. Rohwerder, K. Landfester and D. Crespy, Redox responsive release of hydrophobic self-healing agents from polyaniline capsules, *J. Am. Chem. Soc.*, 2013, **135**(38), 14198–14205, DOI: [10.1021/ja405279t](https://doi.org/10.1021/ja405279t).
- 100 H. Lu, Y. Li, Q. Chen, L. Chen, N. Zhang and M. Ma, Semicrystalline conductive hydrogels for high-energy and stable flexible supercapacitors, *ACS Appl. Energy Mater.*, 2019, **2**(11), 8163–8172, DOI: [10.1021/acsaem.9b01629](https://doi.org/10.1021/acsaem.9b01629).
- 101 W. Liang, S. Rhodes, J. Zheng, X. Wang and J. Fang, Soft-Templated synthesis of lightweight, elastic, and conductive nanotube aerogels, *ACS Appl. Mater. Interfaces*, 2018, **10**(43), 37426–37433, DOI: [10.1021/acsaami.8b14071](https://doi.org/10.1021/acsaami.8b14071).
- 102 Y. Ma, Z. Zhuang, M. Ma, Y. Yang, W. Li, J. Lin, M. Dong, S. Wu, T. Ding and Z. Guo, Solid polyaniline dendrites consisting of high aspect ratio branches self-assembled using sodium lauryl sulfonate as soft templates: Synthesis and electrochemical performance, *Polymer*, 2019, **121**, 121808, DOI: [10.1016/j.polymer.2019.121808](https://doi.org/10.1016/j.polymer.2019.121808).
- 103 J. Liao, S. Wu, Z. Yin, S. Huang, C. Ning, G. Tan and P. K. Chu, Surface-Dependent self-assembly of conducting polypyrrole nanotube arrays in template-free electrochemical polymerization, *ACS Appl. Mater. Interfaces*, 2014, **6**(14), 10946–10951, DOI: [10.1021/am5017478](https://doi.org/10.1021/am5017478).
- 104 P. Worakitsiri, O. Pornsunthorntawe, T. Thanpitcha, S. Chavadej, C. Weder and R. Rujiravanit, Synthesis of polyaniline nanofibers and nanotubes via rhamnolipid biosurfactant templating, *Synth. Met.*, 2011, **161**(3–4), 298–306, DOI: [10.1016/j.synthmet.2010.11.039](https://doi.org/10.1016/j.synthmet.2010.11.039).





- 105 L. Zhang, Y. Long, Z. Chen and M. Wan, The effect of hydrogen bonding on self-assembled polyaniline nanostructures, *Adv. Funct. Mater.*, 2004, **14**(7), 693–698, DOI: [10.1002/adfm.200305020](#).
- 106 C. Laslau, Z. Zujovic and J. Travas-Sejdic, Theories of polyaniline nanostructure self-assembly: Towards an expanded, comprehensive multi-layer theory (MLT), *Prog. Polym. Sci.*, 2010, **35**(12), 1403–1419, DOI: [10.1016/j.progpolymsci.2010.08.002](#).
- 107 S. Guo, Q. Meng, J. Qin, Y. Du, L. Wang, P. Eklund and A. Le Febvrier, Thermoelectric characteristics of self-supporting WSe<sub>2</sub>-nanosheet/PEDOT-nanowire composite Films, *ACS Appl. Mater. Interfaces*, 2023, **15**(29), 35430–35438, DOI: [10.1021/acsami.3c02660](#).
- 108 K. Zhang, J. Qiu and S. Wang, Thermoelectric properties of PEDOT nanowire/PEDOT hybrids, *Nanoscale*, 2016, **8**(15), 8033–8041, DOI: [10.1039/C5NR08421K](#).
- 109 J. Zhang, K. Zhang, F. Xu, S. Wang and Y. Qiu, Thermoelectric transport in ultrathin poly(3,4-ethylenedioxythiophene) nanowire assembly, *Compos. Part B: Eng.*, 2018, **136**, 234–240, DOI: [10.1016/j.compositesb.2017.10.037](#).
- 110 X. Hu, G. Chen, X. Wang and H. Wang, Tuning thermoelectric performance by nanostructure evolution of a conducting polymer, *J. Mater. Chem. A*, 2015, **3**(42), 20896–20902, DOI: [10.1039/C5TA07381B](#).
- 111 J. K. Kawasaki and C. B. Arnold, Synthesis of platinum dendrites and nanowires *via* directed electrochemical nanowire assembly, *Nano Lett.*, 2011, **11**(2), 781–785, DOI: [10.1021/nl1039956](#).
- 112 A. E. Valera, N. T. Nesbitt, M. M. Archibald, M. J. Naughton and T. C. Chiles, On-Chip electrochemical detection of cholera using a polypyrrole-functionalized dendritic gold sensor, *ACS Sens.*, 2019, **4**(3), 654–659, DOI: [10.1021/acssensors.8b01484](#).
- 113 Y. Li, H. Hu, T. Salim, G. Cheng, Y. M. Lam and J. Ding, Flexible wet-spun PEDOT:PSS microfibers integrating thermal-sensing and Joule heating functions for smart textiles, *Polymers*, 2023, **15**(16), 3432, DOI: [10.3390/polym15163432](#).
- 114 J. Yu, R. Wan, F. Tian, J. Cao, W. Wang, Q. Liu, H. Yang, J. Liu, X. Liu, T. Lin, J. Xu and B. Lu, 3D Printing of robust high-performance conducting polymer hydrogel-based electrical bioadhesive interface for soft bioelectronics, *Small*, 2024, **20**(19), 2308778, DOI: [10.1002/smll.202308778](#).
- 115 X. Zhou, S. Fang, Y. Hu, X. Du, H. Ding, R. Chai, J. Han, J. Xie and Z. Gu, Photoinduced double hydrogen-atom transfer for polymerization and 3D printing of conductive polymer, *Nat. Synth.*, 2024, **3**(9), 1145–1157, DOI: [10.1038/s44160-024-00582-w](#).
- 116 Y. Ding, J. Li, X. Qiu, Z. Lin, Y. Zhao, H. Yan, X. Hu and H. Bai, 3D printable polymeric composite material with enhanced conductivity achieved by affinity matching, *ACS Appl. Mater. Interfaces*, 2024, **16**(44), 61016–61025, DOI: [10.1021/acsami.4c13416](#).
- 117 Y. Han, M. Sun, X. Lu, K. Xu, M. Yu, H. Yang and J. Yin, A 3D printable gelatin methacryloyl/chitosan hydrogel assembled with conductive PEDOT for neural tissue engineering, *Compos. Part B: Eng.*, 2024, **273**, 111241, DOI: [10.1016/j.compositesb.2024.111241](#).
- 118 K. Rana, Solution spun electrically conductive nylon 6/poly(pyrrole) nanotubes-based composite fibers, *Synth. Met.*, 2024, **303**, 117550, DOI: [10.1016/j.synthmet.2024.117550](#).
- 119 W. Liu, Y.-C. Chang, J. Zhang and H. Liu, Wet-Spun side-by-side electrically conductive composite fibers, *ACS Appl. Electron. Mater.*, 2022, **4**(4), 1979–1988, DOI: [10.1021/acsaelm.2c00150](#).
- 120 Z. Wang, X. Song, Y. Cui, K. Cheng, X. Tian, M. Dong and L. Liu, Silk fibroin h-fibroin/poly(epsilon-caprolactone) core-shell nanofibers with enhanced mechanical property and long-term drug release, *J. Colloid Interface Sci.*, 2021, **593**, 142–151, DOI: [10.1016/j.jcis.2021.02.099](#).
- 121 A. G. MacDiarmid, W. E. Jones, I. D. Norris, J. Gao, A. T. Johnson, N. J. Pinto, J. Hone, B. Han, F. K. Ko, H. Okuzaki and M. Llaguno, Electrostatically-Generated nanofibers of electronic polymers, *Synth. Met.*, 2001, **119**(1–3), 27–30, DOI: [10.1016/S0379-6779\(00\)00597-X](#).
- 122 T. S. Kang, S. W. Lee, J. Joo and J. Y. Lee, Electrically conducting polypyrrole fibers spun by electrospinning, *Synth. Met.*, 2005, **153**(1–3), 61–64, DOI: [10.1016/j.synthmet.2005.07.135](#).
- 123 L. Xia, Z. Wei and M. Wan, Conducting polymer nanostructures and their application in biosensors, *J. Colloid Interface Sci.*, 2010, **341**(1), 1–11, DOI: [10.1016/j.jcis.2009.09.029](#).
- 124 P. M. George, R. Saigal, M. W. Lawlor, M. J. Moore, D. A. LaVan, R. P. Marini, M. Selig, M. Makhni, J. A. Burdick, R. Langer and D. S. Kohane, Three-Dimensional conductive constructs for nerve regeneration, *J. Biomed. Mater. Res., Part A*, 2009, **91A**(2), 519–527, DOI: [10.1002/jbm.a.32226](#).
- 125 M. Ryu, J. H. Yang, Y. Ahn, M. Sim, K. H. Lee, K. Kim, T. Lee, S.-J. Yoo, S. Y. Kim, C. Moon, M. Je, J.-W. Choi, Y. Lee and J. E. Jang, Enhancement of interface characteristics of neural probe based on graphene, ZnO nanowires, and conducting polymer PEDOT, *ACS Appl. Mater. Interfaces*, 2017, **9**(12), 10577–10586, DOI: [10.1021/acsami.7b02975](#).
- 126 M. Wan, A template-free method towards conducting polymer nanostructures, *Adv. Mater.*, 2008, **20**(15), 2926–2932, DOI: [10.1002/adma.200800466](#).
- 127 Y. Liu, J. H. Xin, X. Zhang and C. Zhang, Morphological evolution of carbon nanotubes synthesized by using conducting polymer nanofibers, *Int. J. Polym. Sci.*, 2020, **2020**, 1–8, DOI: [10.1155/2020/4953652](#).
- 128 J. Jang and H. Yoon, Facile fabrication of polypyrrole nanotubes using reverse microemulsion polymerization—Electronic supplementary information (ESI) available: FTIR spectrum and TEM Images of PPy nanotubes, *Chem. Commun.*, 2003, 720–721, DOI: [10.1039/b211716a](#).
- 129 G. Li and Z. Zhang, Synthesis of dendritic polyaniline nanofibers in a surfactant gel, *Macromolecules*, 2004, **37**(8), 2683–2685, DOI: [10.1021/ma035891k](#).





- 130 S. Yu, F. Qin and G. Wang, Improving the dielectric properties of poly(vinylidene fluoride) composites by using poly(vinyl pyrrolidone)-encapsulated polyaniline nanorods, *J. Mater. Chem. C*, 2016, **4**(7), 1504–1510, DOI: [10.1039/C5TC04026D](#).
- 131 N. Nuraje, K. Su, N. Yang and H. Matsui, Liquid/Liquid interfacial polymerization to Grow single crystalline nanoneedles of various conducting polymers, *ACS Nano*, 2008, **2**(3), 502–506, DOI: [10.1021/nn7001536](#).
- 132 Z. D. Zujovic and J. B. Metson, Nanostructured aniline oxidation products: Self-Assembled films at the air/liquid interface, *Langmuir*, 2011, **27**(12), 7776–7782, DOI: [10.1021/la102684d](#).
- 133 Y. Huang, H. Li, Z. Wang, M. Zhu, Z. Pei, Q. Xue, Y. Huang and C. Zhi, Nanostructured polypyrrole as a flexible electrode material of supercapacitor, *Nano Energy*, 2016, **22**, 422–438, DOI: [10.1016/j.nanoen.2016.02.047](#).
- 134 X. Tan, C. Hu, X. Li, H. Liu and J. Qu, Reversible superwettability switching of a conductive polymer membrane for oil-water separation and self-cleaning, *J. Membr. Sci.*, 2020, **605**, 118088, DOI: [10.1016/j.memsci.2020.118088](#).
- 135 S. Kesornsit, C. Direksilp, K. Phasuksom, N. Thummarungsan, P. Sakunpongpitiporn, K. Rotjanasuworapong, A. Sirivat and S. Niamlang, Synthesis of highly conductive poly(3-hexylthiophene) by chemical oxidative polymerization using surfactant templates, *Polymers*, 2022, **14**(18), 3860, DOI: [10.3390/polym14183860](#).
- 136 P. S. Thapa, B. J. Ackerson, D. R. Grischkowsky and B. N. Flanders, Directional growth of metallic and polymeric nanowires, *Nanotechnology*, 2009, **20**(23), 235307, DOI: [10.1088/0957-4484/20/23/235307](#).
- 137 D. Esrafilzadeh, J. Razal, S. Moulton, E. Stewart and G. Wallace, Multifunctional conducting fibres with electrically controlled release of ciprofloxacin, *J. Controlled Release*, 2013, **169**(3), 313–320, DOI: [10.1016/j.jconrel.2013.01.022](#).
- 138 G. Kiran Raj, E. Singh, U. Hani, K. V. R. N. S. Ramesh, S. Talath, A. Garg, K. Savadatti, T. Bhatt, K. Madhuchandra and R. A. M. Osmani, Conductive polymers and composites-based systems: An incipient stride in drug delivery and therapeutics realm, *J. Controlled Release*, 2023, **355**, 709–729, DOI: [10.1016/j.jconrel.2023.02.017](#).
- 139 A. Puiggali-Jou, L. J. Del Valle and C. Alemán, Drug delivery systems based on intrinsically conducting polymers, *J. Controlled Release*, 2019, **309**, 244–264, DOI: [10.1016/j.jconrel.2019.07.035](#).
- 140 N. Alizadeh and E. Shamaeli, Electrochemically controlled release of anticancer drug methotrexate using nanostructured polypyrrole modified with cetylpyridinium: Release kinetics investigation, *Electrochim. Acta*, 2014, **130**, 488–496, DOI: [10.1016/j.electacta.2014.03.055](#).
- 141 H. Lee, W. Hong, S. Jeon, Y. Choi and Y. Cho, Electroactive polypyrrole nanowire arrays: Synergistic effect of cancer treatment by on-demand drug release and photothermal therapy, *Langmuir*, 2015, **31**(14), 4264–4269, DOI: [10.1021/acs.langmuir.5b00534](#).
- 142 X. Ru, W. Shi, X. Huang, X. Cui, B. Ren and D. Ge, Synthesis of polypyrrole nanowire network with high adenosine triphosphate release efficiency, *Electrochim. Acta*, 2011, **56**(27), 9887–9892, DOI: [10.1016/j.electacta.2011.08.063](#).
- 143 B. C. Thompson, R. T. Richardson, S. E. Moulton, A. J. Evans, S. O'Leary, G. M. Clark and G. G. Wallace, Conducting polymers, dual neurotrophins and pulsed electrical stimulation—dramatic effects on neurite outgrowth, *J. Controlled Release*, 2010, **141**(2), 161–167, DOI: [10.1016/j.jconrel.2009.09.016](#).
- 144 B. C. Thompson, S. E. Moulton, J. Ding, R. Richardson, A. Cameron, S. O'Leary, G. G. Wallace and G. M. Clark, Optimising the incorporation and release of a neurotrophic factor using conducting polypyrrole, *J. Controlled Release*, 2006, **116**(3), 285–294, DOI: [10.1016/j.jconrel.2006.09.004](#).
- 145 C. Chen, X. Chen, H. Zhang, Q. Zhang, L. Wang, C. Li, B. Dai, J. Yang, J. Liu and D. Sun, Electrically-Responsive core-shell hybrid microfibers for controlled drug release and cell culture, *Acta Biomater.*, 2017, **55**, 434–442, DOI: [10.1016/j.actbio.2017.04.005](#).
- 146 Y. Fang, N. Qiao, H. Deng, M. Ren, Y. Zhang, D. Zhang, H. Lin, Y. Chen, K. T. Yong and J. Xiong, PEDOT: PSS-Based microfluidic-spun microfibers for tunable release of acetaminophen via electrical stimulation, *Adv. Mater. Technol.*, 2022, **7**(10), 2200103, DOI: [10.1002/admt.202200103](#).
- 147 B. Lago, M. Brito, C. M. M. Almeida, I. Ferreira and A. C. Baptista, Functionalisation of electrospun cellulose acetate membranes with PEDOT and PPy for electronic controlled drug release, *Nanomaterials*, 2023, **13**(9), 1493, DOI: [10.3390/nano13091493](#).
- 148 D. M. Loh, M. Nava and D. G. Nocera, Polypyrrole-Silicon nanowire arrays for controlled intracellular cargo delivery, *Nano Lett.*, 2022, **22**(1), 366–371, DOI: [10.1021/acs.nanolett.1c04033](#).
- 149 J. Qu, X. Zhao, P. X. Ma and B. Guo, Injectable antibacterial conductive hydrogels with dual response to an electric field and pH for localized “smart” drug release, *Acta Biomater.*, 2018, **72**, 55–69, DOI: [10.1016/j.actbio.2018.03.018](#).
- 150 S. Paramshetti, M. Angolkar, A. Al Fatease, S. M. Alshahrani, U. Hani, A. Garg, G. Ravi and R. A. M. Osmani, Revolutionizing drug delivery and therapeutics: The biomedical applications of conductive polymers and composites-based systems, *Pharmaceutics*, 2023, **15**(4), 1204, DOI: [10.3390/pharmaceutics15041204](#).
- 151 S. E. Moulton, M. J. Higgins, R. M. I. Kapsa and G. G. Wallace, Organic bionics: A new dimension in neural communications, *Adv. Funct. Mater.*, 2012, **22**(10), 2003–2014, DOI: [10.1002/adfm.201102232](#).
- 152 E. Fournier, C. Passirani, C. N. Montero-Menei and J. P. Benoit, Biocompatibility of implantable synthetic polymeric drug carriers: Focus on brain biocompatibility, *Biomaterials*, 2003, **24**(19), 3311–3331, DOI: [10.1016/S0142-9612\(03\)00161-3](#).



- 153 E. Kim, J. Lai, L. Michalek, W. Wang, C. Xu, H. Lyu, W. Yu, H. Park, Y. Tomo, S. E. Root, B. Lee, J. Park, B. Park, S. Wei, C. Zhao and Z. Bao, A transparent, patternable, and stretchable conducting polymer solid electrode for dielectric elastomer actuators, *Adv. Funct. Mater.*, 2025, 35(1), 2411880, DOI: [10.1002/adfm.202411880](https://doi.org/10.1002/adfm.202411880).
- 154 E. A. Cuttaz, C. A. R. Chapman, O. Syed, J. A. Goding and R. A. Green, Stretchable, fully polymeric electrode arrays for peripheral nerve stimulation, *Adv. Sci.*, 2021, 8(8), 2004033, DOI: [10.1002/advs.202004033](https://doi.org/10.1002/advs.202004033).
- 155 M. Yang, L. Wang, W. Liu, W. Li, Y. Huang, Q. Jin, L. Zhang, Y. Jiang and Z. Luo, Highly-Stable, injectable, conductive hydrogel for chronic neuromodulation, *Nat. Commun.*, 2024, 15(1), 7993, DOI: [10.1038/s41467-024-52418-y](https://doi.org/10.1038/s41467-024-52418-y).
- 156 J. Zhang, L. Wang, Y. Xue, I. M. Lei, X. Chen, P. Zhang, C. Cai, X. Liang, Y. Lu and J. Liu, Engineering electrodes with robust conducting hydrogel coating for neural recording and modulation, *Adv. Mater.*, 2023, 35(3), 2209324, DOI: [10.1002/adma.202209324](https://doi.org/10.1002/adma.202209324).
- 157 S. Kim, D. Yoo and J. Kim, Mechanically robust 3D flexible electrodes *via* embedding conductive nanomaterials in the surface of polymer networks, *Small Methods*, 2025, 2401839, DOI: [10.1002/smt.202401839](https://doi.org/10.1002/smt.202401839).
- 158 J. Zhang, X. Zhang, C. Wang, F. Li, Z. Qiao, L. Zeng, Z. Wang, H. Liu, J. Ding and H. Yang, Conductive composite fiber with optimized alignment guides neural regeneration under electrical stimulation, *Adv. Healthcare Mater.*, 2021, 10(3), 2000604, DOI: [10.1002/adhm.202000604](https://doi.org/10.1002/adhm.202000604).
- 159 F. Xiong, S. Wei, S. Wu, W. Jiang, B. Li, H. Xuan, Y. Xue and H. Yuan, Aligned electroactive electrospun fibrous scaffolds for peripheral nerve regeneration, *ACS Appl. Mater. Interfaces*, 2023, 15(35), 41385–41402, DOI: [10.1021/acsami.3c09237](https://doi.org/10.1021/acsami.3c09237).
- 160 S. Song, K. W. McConnell, D. Amores, A. Levinson, H. Vogel, M. Quarta, T. A. Rando and P. M. George, Electrical stimulation of human neural stem cells *via* conductive polymer nerve guides enhances peripheral nerve recovery, *Biomaterials*, 2021, 275, 120982, DOI: [10.1016/j.biomaterials.2021.120982](https://doi.org/10.1016/j.biomaterials.2021.120982).
- 161 D. Xu, L. Fan, L. Gao, Y. Xiong, Y. Wang, Q. Ye, A. Yu, H. Dai, Y. Yin, J. Cai and L. Zhang, Micro-Nanostructured polyaniline assembled in cellulose matrix *via* interfacial polymerization for applications in nerve regeneration, *ACS Appl. Mater. Interfaces*, 2016, 8(27), 17090–17097, DOI: [10.1021/acsami.6b03555](https://doi.org/10.1021/acsami.6b03555).
- 162 H. Yang, G. Zhu, Y. Huang, X. Shi and Y. Wang, The stimulation of the differentiation of pheochromocytoma (PC12-L) cells into neuron-like cells by electrically conductive nanofibre mesh, *Appl. Mater. Today*, 2016, 5, 215–222, DOI: [10.1016/j.apmt.2016.09.017](https://doi.org/10.1016/j.apmt.2016.09.017).
- 163 X. Hu, X. Wang, Y. Xu, L. Li, J. Liu, Y. He, Y. Zou, L. Yu, X. Qiu and J. Guo, Electric conductivity on aligned nanofibers facilitates the transdifferentiation of mesenchymal stem cells into schwann cells and regeneration of injured peripheral nerve, *Adv. Healthcare Mater.*, 2020, 9(11), 1901570, DOI: [10.1002/adhm.201901570](https://doi.org/10.1002/adhm.201901570).
- 164 J. Xue, J. Yang, D. M. O'Connor, C. Zhu, D. Huo, N. M. Boulis and Y. Xia, Differentiation of bone marrow stem cells into schwann cells for the promotion of neurite outgrowth on electrospun fibers, *ACS Appl. Mater. Interfaces*, 2017, 9(14), 12299–12310, DOI: [10.1021/acsami.7b00882](https://doi.org/10.1021/acsami.7b00882).
- 165 S. Wang, H. Lu, X. Kang, Z. Wang, S. Yan, X. Zhang and X. Shi, Electroconductive and Immunomodulatory Natural Polymer-Based Hydrogel Bandages Designed for Peripheral Nerve Regeneration, *Adv. Funct. Mater.*, 2024, 34(8), 2310903, DOI: [10.1002/adfm.202310903](https://doi.org/10.1002/adfm.202310903).
- 166 A. Farzan, S. Borandeh and J. Seppälä, Conductive Polyurethane/PEGylated Graphene Oxide Composite for 3D-Printed Nerve Guidance Conduits, *Eur. Polym. J.*, 2022, 167, 111068, DOI: [10.1016/j.eurpolymj.2022.111068](https://doi.org/10.1016/j.eurpolymj.2022.111068).
- 167 K. Liu, S. Yan, Y. Liu, J. Liu, R. Li, L. Zhao and B. Liu, Conductive and alignment-optimized porous fiber conduits with electrical stimulation for peripheral nerve regeneration, *Mater. Today Bio*, 2024, 26, 101064, DOI: [10.1016/j.mtbio.2024.101064](https://doi.org/10.1016/j.mtbio.2024.101064).
- 168 Y. Jiang, M. Xu and V. K. Yadavalli, Silk fibroin-sheathed conducting polymer wires as organic connectors for biosensors, *Biosensors*, 2019, 9(3), 103, DOI: [10.3390/bios9030103](https://doi.org/10.3390/bios9030103).
- 169 M. Naseri, L. Fotouhi and A. Ehsani, Recent progress in the development of conducting polymer-based nanocomposites for electrochemical biosensors applications: A mini-review, *Chem. Rec.*, 2018, 18(6), 599–618, DOI: [10.1002/tcr.201700101](https://doi.org/10.1002/tcr.201700101).
- 170 A. Soni, C. M. Pandey, S. Solanki, R. K. Kotnala and G. Sumana, Electrochemical genosensor based on template assisted synthesized polyaniline nanotubes for chronic myelogenous leukemia detection, *Talanta*, 2018, 187, 379–389, DOI: [10.1016/j.talanta.2018.05.038](https://doi.org/10.1016/j.talanta.2018.05.038).
- 171 X. Wang, X. Wang, X. Wang, F. Chen, K. Zhu, Q. Xu and M. Tang, Novel electrochemical biosensor based on functional composite nanofibers for sensitive detection of P53 tumor suppressor gene, *Anal. Chim. Acta*, 2013, 765, 63–69, DOI: [10.1016/j.aca.2012.12.037](https://doi.org/10.1016/j.aca.2012.12.037).
- 172 X. Sun, N. Hui and X. Luo, Reagentless and label-free voltammetric immunosensor for carcinoembryonic antigen based on polyaniline nanowires grown on porous conducting polymer composite, *Microchim. Acta*, 2017, 184(3), 889–896, DOI: [10.1007/s00604-016-2068-0](https://doi.org/10.1007/s00604-016-2068-0).
- 173 D. Wang and J. Wang, A sensitive and label-free electrochemical microRNA biosensor based on polyamidoamine dendrimer functionalized polypyrrole nanowires hybrid, *Microchim. Acta*, 2021, 188(5), 173, DOI: [10.1007/s00604-021-04824-y](https://doi.org/10.1007/s00604-021-04824-y).
- 174 Y. Jing, A. Wang, J. Li, Q. Li, Q. Han, X. Zheng, H. Cao and S. Bai, Preparation of conductive and transparent dipeptide hydrogels for wearable biosensor, *Bio-Des. Manuf.*, 2022, 5(1), 153–162, DOI: [10.1007/s42242-021-00143-6](https://doi.org/10.1007/s42242-021-00143-6).
- 175 A. Keirouz, Y. L. Mustafa, J. G. Turner, E. Lay, U. Jungwirth, F. Marken and H. S. Leese, Conductive polymer-coated 3D



- printed microneedles: biocompatible platforms for minimally invasive biosensing interfaces, *Small*, 2023, **19**(14), 2206301, DOI: [10.1002/sml.202206301](https://doi.org/10.1002/sml.202206301).
- 176 X. Wang, M. Xu, H. Yang, W. Jiang, J. Jiang, D. Zou, Z. Zhu, C. Tao, S. Ni, Z. Zhou, L. Sun, M. Li, Y. Nie, Y. Zhao, F. He, T. H. Tao and X. Wei, Ultraflexible neural electrodes enabled synchronized long-term dopamine detection and wideband chronic recording deep in brain, *ACS Nano*, 2024, **18**(50), 34272–34287, DOI: [10.1021/acsnano.4c12429](https://doi.org/10.1021/acsnano.4c12429).
- 177 T. Xu, W. Ji, X. Wang, Y. Zhang, H. Zeng, L. Mao and M. Zhang, Support-Free PEDOT:PSS fibers as multifunctional microelectrodes for *in vivo* neural recording and modulation, *Angew. Chem., Int. Ed.*, 2022, **61**(16), e202115074, DOI: [10.1002/anie.202115074](https://doi.org/10.1002/anie.202115074).
- 178 J. Ni, H. Wei, W. Ji, Y. Xue, F. Zhu, C. Wang, Y. Jiang and L. Mao, Aptamer-Based potentiometric sensor enables highly selective and neurocompatible neurochemical sensing in rat brain, *ACS Sens.*, 2024, **9**(5), 2447–2454, DOI: [10.1021/acssensors.4c00119](https://doi.org/10.1021/acssensors.4c00119).

